Russian Chemical Reviews **68** (9) 709 – 726 (1999) © 1999 Russian Academy of Sciences and Turpion Ltd

UDC 539.143.44 + 541.49 + 541.67

Electronic effects of substitution and reconstruction of the coordination polyhedron in adducts of Main Group IV element halides

E A Kravchenko, Yu A Buslaev

Contents

I.	Introduction	709
II.	Electronic effects of substitution in adducts of tin(IV) halides	710
III.	Electronic characteristics of M – Hal bonds in hexa- and pentacoordinate adducts of tin(IV) tetrachlorides; similarities and differences	717
IV.	Penta- and hexacoordinate adducts of silicon and germanium tetrachlorides	721
V.	Conclusion	725

Abstract. Nuclear quadrupole resonance and X-ray data on the electronic effects of substitution of acidoligands and reconstruction of the coordination polyhedra in adducts (complexes) of tin(IV), germanium(IV) and silicon(IV) tetrahalides due to the change in the central metal coordination number are surveyed and systematically described. The σ- and π-electron density redistribution over the central metal – halogen bonds resulting from substitution or reconstruction of the coordination polyhedra from pseudooctahedral to trigonal-bipyramidal geometry is discussed. The bibliography includes 55 references.

I. Introduction

Redistribution of electron density upon substitution or reconstruction of the central atom coordination polyhedron in coordination compounds is a fundamental problem of the chemistry and stereochemistry of heteroligand complexes. Whereas the importance of this problem in the coordination chemistry of transition elements is widely known, the electronic effects in the chemistry of main group elements have been studied less extensively. Electronic effects of substitution as well as their steric manifestations are extremely diverse in such compounds, the resulting changes in the metal – halogen bonds being sensitive to details of the electronic structure of the whole adduct, *viz*., the central metal, ligands and substituents. In most earlier publications, the electronic mechanism of substituent influence was discussed based on the position of ligands in various rows, AO occupancies determined by approximate quantum-chemical calculations and X-ray data. However, all these characteristics related only indirectly to the phenomenon in question, because the contribution of the substituents to the changes in the appropriate parameters is as a rule not unique and sometimes not predominant. Often, the results thus obtained do not allow determination of both the extent of the influence and even its direction. As a result, many important questions of the electronic mechanism of ligand influence in main group element coordination compounds remain still open. In particular, quantitative data on electron density redistribution over the atomic σ and π orbitals as a result of either substitution of acidoligands or change in the adduct geometry, caused by the change in the central atom coordination number, were very scanty.

The intention of this review is to bring to the attention of researchers a feasibility of quantitative description of electron density redistribution in Main Group IV element coordination compounds using nuclear quadrupole resonance (NQR) spectroscopic data. Here we discuss only static influence of substituents, which reflects processes in a system in the ground state. In this case, a parameter can be used as a measure of substituent (ligand) electronic influence if it satisfies at least two requirements: first, it characterises a system in its ground state and second, it is changed predominantly under this influence. In this respect, NQR spectroscopic parameters seem to be quite suitable, since they are the ground-state characteristics of a system directly relating to the electron density distribution in the vicinity of a quadrupolar nucleus.

NQR spectroscopy investigates interactions between nuclei having nonzero quadrupole moment Q (all the nuclei with spin $I > 1/2$ have such a moment) and their local electric environment. The latter is characterised by the electric field gradient (EFG)

$$q_{ij} = \frac{\partial E_i}{\partial j} = \frac{\partial^2 U}{\partial ij},$$

where E_i is the strength of the electrostatic field, U is the electrostatic potential at the nuclear site and $i, j = x, y, z$. The directly measured spectroscopic parameters are the quadrupole coupling constant (QCC)

$$\mathrm{QCC} = \frac{e^2 Q q_{zz}}{h},$$

where e is the charge on the electron and h is the Planck constant, and the EFG asymmetry parameter

$$\eta = \frac{|q_{xx} - q_{yy}|}{q_{zz}}.$$

Because the values of QCC and η depend directly on the electron density distribution around the nucleus under study, any weak disturbance of the electron density upon indroduction of a substituent is clearly reflected in the NQR spectra. The physical

E A Kravchenko, Yu A Buslaev N S Kurnakov Institute of General and Inorganic Chemistry, Russian Academy of Sciences, Leninsky prosp., 117907 Moscow, Russian Federation. Fax (7-095) 954 12 79. E-mail: ekravch@ionchran.rinet.ru (E A Kravchenko). Tel. (7-095) 952 22 78. E-mail: buslaev@ionchran.rinet.ru (Yu A Buslaev)

Received 1 December 1998
Uspekhi Khimii **68** (9) 787 – 805 (1999); translated by E A Kravchenko

principles of the NQR phenomenon, the scope and limitations of NQR spectroscopy in application to problems of inorganic and coordination chemistry have been reviewed.[1]

X-Ray diffraction analysis is yet another approach to the study of substituent effects. However, one should bear in mind that the changes in interatomic distances depend on numerous factors which form the optimum crystal packing and are not necessarily related to the effects of substitution. Comparison of NQR and X-ray data allows one to determine the changes in effective charge on atoms upon the appropriate bond lengthening, which, in turn, helps to outline the range of variation of interatomic distances under the influence of substituents. The use of the two experimental techniques providing complementary pieces of information, on such important properties of compounds as electron density distribution and spatial arrangement of atoms, permits avoiding indirect estimations in the study of the problem on a quantitative level.

This review presents the results of NQR spectroscopic studies on the σ- and π-electron density redistribution over metal–halogen bonds in tin(IV), germanium(IV) and silicon(IV) halide complexes and adducts resulting from the substitution and/or change in the central atom coordination number. The following series are considered: $MHal_4 \rightarrow MHal_4L \rightarrow MHal_4L_2$, $SnHal_4L_2 \rightarrow R_nSnHal_{4-n}L_2$ and $[SnHal_6]^{2-} \rightarrow [RSnHal_5]^{2-}$, where M = Sn, Ge and Si; Hal = Cl, Br and I; R = Alk and Ph; and L are oxygen- and nitrogen-containing ligands.

II. Electronic effects of substitution in adducts of tin(IV) halides

The problem of electron density redistribution over the atomic σ and π orbitals of metal–halogen bonds upon substitution in tin(IV) adducts of the type $SnHal_4L_2$ ($[SnHal_6]^{2-}$)→ $R_nSnHal_{4-n}L_2$ ($[RSnHal_5]^{2-}$) seems to be most intriguing. The solution of this problem requires the knowledge of the complete set of NQR spectroscopic parameters for the complexes and adducts of parent tin tetrahalides including the asymmetry parameters η of the halogen atoms. In this respect, iodostannates are most suitable for NQR studies, because the iodine (^{127}I) nuclear spin is $I = 5/2$ and the QCC and values in the iodo adducts can be found, provided both resonance transition frequencies, ν_1 ($\Delta m = 1/2-3/2$) and ν_2 ($\Delta m = 3/2-5/2$) are observed.[1] No additional experiments are necessary in this case, whereas they are necessary for determining η in chlorostannates, because only two degenerate quadrupole levels and one transition frequency are available for chlorine nuclei with $I = 3/2$, which precludes simultaneous determination of the QCC and η values from the known relationship

$$\nu = \frac{e^2 Q q_{zz}}{2h(1+\eta^2/3)^{1/2}} .$$

The EFG asymmetry parameter provides additional information on the electron density distribution around the nucleus in question, because η is a measure of the bonding electron cloud axial asymmetry. Hence the problem of measuring η on the $^{35,37}Cl$ nuclei with $I = 3/2$, which are most often subject to NQR studies, is considered by spectroscopists as being of current interest, and various attempts were undertaken to solve it. Most determinations of η on the ^{35}Cl atoms were made by Zeeman studies of single crystals.[1,2] These measurements provide high precision of the η values and permit determination of the orientation of the EFG axes with respect to the crystallographic axes of the specimen. However, this approach substantially reduces the number of the compounds that can be examined, eliminating those air- or moisture-sensitive as well as presenting problems for the crystal growth.

The number of reports on the determination of η in crystalline powders is much less. The majority of the results published by foreign authors were obtained using the CW technique, which as a rule gives low accuracy of measurements[2]. The advantages of pulsed methods over stationary ones for measuring η in powders were outlined in the review.[1] One approach was based on the Fourier-analysis of slow beats of the spin echo envelope in external magnetic fields of 15–100 Œ. In powders of chlorine-containing compounds, this provided values of η in reasonable agreement with those available for the appropriate single crystals.[3] This approach was applied for determination of η in organic and organoelement compounds.[4–7] Later, it was modified[8] to be used for measuring η in a large number of adducts of tin, germanium and silicon tetrachlorides.[9–12]

The determination of η in compounds in question enables one to escape the σ-approximation, to take into account the electron density distribution over the tin–halogen σ and π orbitals and to juxtapose trends in electron density redistribution upon substitution of different groups for acidoligands. Within the Townes and Dailey theory approximations, the measured NQR spectroscopic parameters (QCC and η) are related to the halogen atom valence *p*-orbital occupancies Npi ($i = x, y, z$) and electronic characteristics of metal–halogen bonds as follows:

$$U_p = \frac{e^2 Q q_{zz}}{e^2 Q q_0} = \left| \frac{Np_x + Np_y}{2} - Np_z \right| = \sigma - \frac{\pi}{2} , \quad (1)$$

$$\eta = \frac{q_{xx} - q_{yy}}{q_{zz}} = \frac{3(Np_x - Np_y)}{2Np_z - (Np_x + Np_y)} = \frac{3(\pi_x - \pi_y)}{2U_p} , \quad (2)$$

where e^2Qq_{zz} is the QCC value at the halogen atom, e^2Qq_0 is the atomic QCC produced by a single electron on the valence p_z orbital of the halogen atom;

$$Np_z = 2 - \sigma,$$
$$Np_x = 2 - \pi_x,$$
$$Np_y = 2 - \pi_y;$$
$$\pi_x + \pi_y = \pi\,;\ i + \sigma + \pi = 1,$$

where i, σ and π are the ionic, covalent and π-character of the bond.

Whereas the mutual ligand influence in similar transition metal compounds is known to alter the metal–halogen bonds in such a way that the *trans*-influence is prevailng and is accompanied by a slight change in the *cis*-bonds, the resulting changes in the Sn–Hal bonds due to the introduction of substituents R into $[SnHal_6]^{2-}$ or $SnHal_4L_2$ were found to be sensitive to details of the electronic structure of the whole adduct, *viz*., to the AO energies for the central atom, the halogen atoms and substituents as well as to the oxidation state of the central atom. Depending on the oxidation state of the central metal and its position in the Periodic Table, *cis*-weakening, or *trans*-weakening or *cis*-weakening accompanied by a relatively smaller *trans*-influence can prevail, both strengthening and weakening being possible in principle. Various theoretical approaches have been developed to describe the effects of substituents (ligands) in main group element complexes.

Based on the model of equivalent orbitals applicable to compounds having covalent two-electron two-centre bonds, the mechanism of ligand influence was described as purely inductive.[13] As a result of substitution, the M–Hal bonds were predicted to undergo changes so as to provide prevailing of *cis*- over *trans*-influence. In the approach using the canonical σ-MO within the perturbation theory approximations, the atomic orbital energies of the halogen ligands and substituents were assumed to be close to each other.[14] According to this approach a *trans*-influence prevailing over relatively weak *cis*-influence was expected as the contribution of the *np* orbitals of the central atom became more pronounced. A consideration which took into account all the transitions between the occupied and vacant MOs suggested that the central atom valence basis set involved mostly *ns* and *np* orbitals rather than the vacant *nd*-AOs.[15] The resulting

change in the the M – Hal bond character upon substitution was determined in this case by a relationship between the energies of the levels for the valence *ns*- and *np*-AOs of the central atom and *s*-AOs of typical ligands. This means that the influence was expected to be essentially different for the compounds of Groups II – IV (type I) and VII (type II) elements. Thus the substitution $[MHal_6]^{2-} \rightarrow [RMHal_5]^{2-}$ in complexes of the Main Group IV element was predicted to result in contraction of the $[MHal_6]^{2-}$ octahedron along the *z* axis and its expansion in equatorial directions, if substituent R is more electropositive than Hal, whereas the octahedron will be expanded along the *z* axis and contracted in the *x*, *y* directions, if R is more electronegative than Hal.

A model of hypervalent (HV) orbital-deficient bonds[16] applied to tin(IV) compounds[17] suggests that the central atom valence basis involves only *ns* and *np* orbitals. According to this model, in the parent $[SnHal_6]^{2-}$ complex, the 5*s* orbitals of the tin atom participate in the formation of three equivalent three-center *sp*-hybrid hypervalent (HV-I) bonds Hal – Sn – Hal, each involving only one 5*p* orbital of the tin atom. The σ-level energies of the substituents R in adducts (complexes) $R_nSnHal_{4-n}L_2$ and $[SnHal_6]^{2-}$ are then close in value to those of the *p* levels of the central atom, while the σ-level energies of the acidoligands are close in value to those of the *s* levels of the tin atom.

In alkyl- and dialkyl-substituted complexes, occupation of a_1^* MOs occurs, which are antibonding with respect to the equatorial ligands. Because the a_1^* MOs contain a remarkable contribution from the *s* orbital of the central atom, the *s*-character of the equatorial bonding orbitals is reduced, so that the corresponding bonds (HV-II) are weakened compared to the bonds HV-I in the parent nonsubstituted complex $[SnHal_6]^{2-}$. On the other hand, alkyl substituents R cannot form stable hypervalent bonds with tin, because R is less electronegative that the tin atom, so that the Alk – Sn bonds are ordinary covalent two-centre two-electron bonds.

Thus, for the adducts and complexes $RSnHal_3L_2$ and $[RSnHal_5]^{2-}$, the model of hypervalent orbital-deficient bonds predicts weakening of the Sn – Hal bonds at the *cis*-position to the alkyl substituent compared to the bonds in the initial $SnHal_4L_2$ or $[SnHal_6]^{2-}$ compounds. The weakening can be accompanied by *trans*-influence, presumably strengthening of the Sn – Hal bond at the *trans*-position to the substituent R.

Using NQR, the electronic effects of substitution were observed experimentally: the direction of the *trans*-influence was determined and the relative importance of the effects of *cis*- and *trans*-influence was quantitatively compared. Most clear manifestations of both effects were obtained for pseudooctahedral complexes of the type $[RSnHal_5]^{2-}$ and molecular adducts $R_nSnHal_{4-n}L_2$ where the tin atom is in its highest oxidation state and either one or two acidoligands (Hal) are substituted for alkyl groups R, which considerably exceed the halogen ligands in donating power. The effects of substitution were especially strong in these compounds, and we discuss here how the substitution influences the σ- and π-electron density distribution in the complexes and molecules of adducts.

Tables 1 and 2 list the NQR spectroscopic parameters measured for the substituted tin(IV) compounds and their unsubstituted precursors, hexahalostannates Cat_2SnHal_6 (Cat is cation) and pseudooctahedral adducts of tin tetrahalides $SnHal_4L_2$. The appropriate Sn – Hal interatomic distances wherever available are also given in these tables. As is seen from Tables 1 and 2, the *cis*- and *trans*-influence of the substituents is clearly reflected in the NQR spectra, which enables one to compare their contribution to the resulting electron density redistribution on a quantitative scale. In Tables 3 and 4, the halogen atom valence p_σ orbital occupancies (Np_z) and p_π orbital occupancy differences ($\Delta Np_\pi = Np_x - Np_y$), estimated from the NQR data, are given for the adducts and complexes of parent unsubstituted and mono- and dialkyl(diphenyl)-substituted tin halides $[RSnHal_5]^{2-}$, $RSnHal_3L_2$, $R_2SnHal_2L_2$. The main sources of inaccuracy in the determination of the spectroscopic parameters as well as the reliability of interpreting the spectral data were discussed in a review.[3] Based on the estimated values of the atomic orbital occupancies, the effective charges (ρ) on the halogen atoms and their variation ($\Delta\rho$) as a result of the introduction of the substituents R were determined

$$\Delta\rho = \frac{\rho(R_nSnHal_{4-n}L_2) - \rho(SnHal_4L_2)}{\rho(SnHal_4L_2)}. \quad (3)$$

Similarly, the variation of the Sn – Hal bond distances (Δd) was estimated in compounds whose structures were studied

$$\Delta d = \frac{d(R_nSnHal_{4-n}L_2) - d(SnHal_4L_2)}{d(SnHal_4L_2)}. \quad (4)$$

The values of Δd are also listed in Tables 3 and 4.

The NQR spectra provide evidence for a profound electron density redistribution upon substitution. The negative effective charge on the halogen atoms in the *cis*-position to the substituent R increases in absolute magnitude with respect to the corresponding parent compounds hence yielding the positive values of $\Delta\rho$ (Tables 3 and 4). On the halogen atoms in the *trans*-position to the substituent, the absolute magnitude of the charge falls as compared to that in the parent nonsubstituted adduct. The negative values of $\Delta\rho$, found for the *trans*-halogens in all the adducts studied, indicate that the *trans*-influence of substituents R always acts in these compounds as *trans*-strengthening of the Sn – Hal bonds. The only exception was the adduct $EtSnCl_3(DMSO)_2$ (Table 3), in which strong donor ligands compensate the effect of *trans*-strengthening (and accordingly *trans*-shortening). The introduction of an ethyl group into a $[SnCl_6]^{2-}$ complex (its singlet NQR spectrum points to the equivalence of all the chlorine atoms) results in the formation of the complex $[EtSnCl_5]^{2-}$ characterised by an NQR spectrum with a spectroscopic splitting of 6 MHz between the frequencies, assigned to the chlorine atoms in *cis*- and *trans*-positions relative to the substituent R. The effective charges on the appropriate chlorine atoms differ on average by 0.1 e. The difference between the characteristics of the *cis*- and *trans*-bromine atoms in the complex $[BuSnBr_5]^{2-}$ is even more pronounced: the splitting of the corresponding ^{81}Br NQR frequencies exceeds 50 MHz, whereas the difference in effective charges on the corresponding Br atoms reaches 0.16 e (see Ref. 3).

It is evident that such values of frequency shifts and spectroscopic splittings are mainly due to the intramolecular electronic rather than crystal-field effects. A correlation between the ^{35}Cl NQR frequencies and Sn – Cl bond lengths was examined for a large number of chlorine-containing tin compounds including hexacoordinate tin(IV) complexes of the types Cat_2SnHal_6 and $Cat_2RSnHal_5$ with various cations and anions, electroneutral adducts of types $SnCl_4L_2$ and $R_2SnCl_2L_2$ and compounds R_nSnCl_{4-n}, where the tin atom is tetracoordinate and both terminal and bridging chlorine atoms are available.[19] Tin(II) compounds $SnCl_2 \cdot xH_2O$ ($x = 0$, 1.5, 2) were also taken into consideration. The results of the analysis showed that the maximum contribution of the crystal field to the frequency shifts and Sn – Cl bond lengths in these compounds does not exceed 2 MHz and 0.05 Å, respectively. These contributions are evidently less in crystallochemically similar chlorine-containing compounds listed in Tables 3 and 4. Their further decrease occurs on going to more covalent tin(IV) bromo- and iodo compounds. It should be added that the relative changes of the effective charges on atoms are considered as the measure of substituent effects rather than their absolute values. Thus the electronic effect of the ethyl substituent in pentachloroethylstannate was estimated from changes in the effective charges on the chlorine atoms compared to those in the parent hexachlorostannate with the same cation, which implies that the crystal field contributions to the ^{35}Cl NQR frequencies of both pentachloroethyl- and hexachloro-stannate are virtually the same.[20,21]

Table 1. ^{35}Cl and ^{81}Br frequencies [$\nu(^{35}Cl)$ and $\nu(^{81}Br)$/MHz], EFG asymmetry parameters (η) in the NQR spectra of $SnHal_4L_2$, $[SnHal_6]^{2-}$, $R_nSnHal_{4-n}L_2$ and $[RSnHal_5]^{2-}$ at 77 K and Sn–Hal bond distances (d).[9–11, 18, 19–22, 23]

Compound	$\nu(^{35}Cl)$	η (%)	d(Sn–Cl) /Å	Assignment	$\nu(^{81}Br)$	η (%)	d(Sn–Br) /Å	Assignment
$(NMe_4)_2SnHal_6$ [a]	16.683	–	2.424(3)	Cl–Sn–Cl	115.07	–	2.605(1)	Br–Sn–Br
$(NMe_4)_2RSnHal_5$ [a]	12.329	{10.0}	2.516(10)	Cl–Sn–Cl	81.94	{10.0}	2.699(5)	Br–Sn–Br
	18.070	–	2.407(3)	Cl–Sn–Et	133.36	–	2.566(2)	Br–Sn–Bu
$(MeNH_3)_2SnCl_6$ [a]	15.815	–	2.417(3)	Cl–Sn–Cl				
$(MeNH_3)_2EtSnCl_5$ [a]	12.072	11.7(3)	2.507(1)	Cl–Sn–Cl				
	11.537	14.6(3)	2.531(1)	Cl–Sn–Cl				
	10.770	15.4(3)	2.497(1)	Cl–Sn–Cl				
	9.969	17.1(3)	2.549(1)	Cl–Sn–Cl				
	17.032	5.6(3)	2.426(1)	Cl–Sn–Et				
$(PyH)_2SnCl_6$ [a]	16.588	–	2.431(1)	Cl–Sn–Cl				
$(PyH)_2EtSnCl_5$ [a]	11.322	{14.0}	2.518(1)	Cl–Sn–Cl				
	17.926	–	2.401(2)	Cl–Sn–Et				
	L = HMPT					L = HMPT		
trans-$SnHal_4L_2$	17.91	10.6	2.388(1)	Cl–Sn–Cl	127.75	{10.6}	2.55(1)	Br–Sn–Br
trans-$RSnHal_3L_2$	20.02	{0–5.0}	2.379(1)	Cl–Sn–Et	132.60	{>6.5}	2.529(1)	Br–Sn–Bu
	–	–	2.491(1)	Cl–Sn–Cl	93.82	{10.6}	2.633(1)	Br–Sn–Br
trans-$PhSnCl_3L_2$	18.525	{>6.7}	–	Cl–Sn–Ph				
	14.045	{10.6}	–	Cl–Sn–Cl				
trans-$Me_2SnHal_2L_2$	9.450	{10.6}	2.570(1)	Cl–Sn–Cl	60.61	{10.6}	2.74(1)	Br–Sn–Br
	L = THF					L = THF		
trans-$SnHal_4L_2$	19.02	13.5	–	Cl–Sn–Cl	132.44	{13.5}	–	Br–Sn–Br
$MeSnHal_3L_2$	20.17	{>7.0}	–	Cl–Sn–Me	141.12	{>6.2}	–	Br–Sn–Me
	15.45	{13.5}	–	Cl–Sn–Cl	104.70	{13.5}	–	Br–Sn–Br
$Me_2SnBr_2L_2$					99.04	{13.5}	–	Br–Sn–Br
	L = TMU					L = TMU		
trans-$SnHal_4L_2$	18.24	7.5	2.391(1)	Cl–Sn–Cl	124.44	{7.5}	–	Br–Sn–Br
trans-$SnHal_3L_2$	19.35	{>1.4}	2.374(4)	Cl–Sn–Et				
	13.47	{7.5}	2.491(4)	Cl–Sn–Cl				
trans-$Et_2SnBr_2L_2$					75.71	{7.5}	–	Br–Sn–Br
	L = DMSO					L = DMSO		
cis-$SnHal_4L_2$	18.36	{3.0}	2.382(3)	Cl–Sn–Cl	118.17	{3.0}	–	Br–Sn–Br
	17.045	{14.0}	2.391(3)	Cl–Sn–O	127.73	{14.0}	–	Br–Sn–O
cis-$EtSnCl_3L_2$	13.52	14.0	2.456(4)	Cl–Sn–O				
	16.96	3.0	2.398(3)	Cl–Sn–Et				
cis-$Me_2SnCl_2L_2$	10.40	{14.0}	2.51(1)	Cl–Sn–O				
trans-$Me_2SnBr_2L_2$					59.46	{14.0}	2.752(1)	Br–Sn–Br
	L = Me_2CO							
cis-$SnHal_4L_2$	19.75	1.2	–	Cl–Sn–Cl				
	19.135	7.0	–	Cl–Sn–O				
	L = DMF							
trans-$SnCl_4L_2$	17.77	5.7	–	Cl–Sn–Cl				
cis-$Me_2SnCl_2L_2$	11.13	{5.7}	2.47(1)	Cl–Sn–O				
						L = DPSO		
cis-$SnBr_4L_2$					116.63	–	2.556(1)	Br–Sn–Br
					128.30	–	2.527(2)	Br–Sn–O
cis-$BuSnBr_3L_2$ [b]					90.72	–	2.627(2)	Br–Sn–Br
					102.40	–	2.559(1)	Br–Sn–O
	L = py					L = py		
trans-$SnHal_4L_2$	17.70	15.4		Cl–Sn–Cl	122.66	{15.4}		Br–Sn–Br
trans-$Me_2SnHal_2L_2$					65.76	{15.4}	2.719(5)	Br–Sn–Br
trans-$Et_2SnHal_2L_2$					64.61	{15.4}	–	Br–Sn–Br
						L = bipy		
cis-$SnBr_4L$					118.87	{0.0}	2.565(1)	Br–Sn–Br
					129.92	{15.4}	2.540(1)	Br–Sn–N
cis-$Bu_2SnBr_2L_2$					74.69	{15.4}	2.714(1)	Br–Sn–N

Note. Resonance frequencies of chemically equivalent halogen atoms are averaged over crystallographically inequivalent positions for all the compounds except for $(MeNH_3)_2EtSnHal_5$. The values expected by analogy with those measured for the related compounds are given in braces. HMPT is hexamethylphosphortriamide; THF is tetrahydrofuran; TMU is tetramethyl urea; DMSO is dimethyl sulfoxide; DMF is dimethylformamide; DPSO is diphenyl sulfoxide; py is pyridine; bipy is bipyridyl.

[a] The NQR data at 300 K. [b] The substituent R (Bu) is in *trans*-position to the ligand DPSO.[24]

Table 2. ^{127}I NQR spectroscopic parameters [ν_1, ν_2, e^2Qq_{zz}/h (MHz); η] for adducts SnI_4L_2 and $R_nSnI_{4-n}L_2$ at 77 K and Sn–I bond distances (d).[12, 18, 25, 26]

Compound	ν_1	ν_2	e^2Qq_{zz}/h	η (%)	d /Å	Assignment
L = HMPT						
cis-SnI_4L_2	156.15	312.15 [a]	1040.59 [a]	{1.9}	–	I–Sn–I
	164.61	327.69 [a]	1093.11 [a]	{6.0}	–	I–Sn–O
cis-$EtSnI_3L_2$	166.40	–	–	–	2.634(4)	I–Sn–Et
	111.30	219.17	732.40	11.0	2.886(2)	I–Sn–O
	109.80	–	–	–	2.901(2)	I–Sn–O
trans-$Et_2SnI_2L_2$	70.51	140.26	467.90	6.5	3.016(1)	I–Sn–I
trans-$Ph_2SnI_2L_2$ (see [b]) (I)	86.92	144.00	495.17	41.2	2.957(1)	I–Sn–I
(II)	88.46	146.60	504.08	41.2	2.938(1)	I–Sn–I
L = TMU						
cis-SnI_4L_2	157.27	314.39	1048.04	1.9	–	I–Sn–I
	164.93	328.35	1095.28	6.0	–	I–Sn–O
L = TPPO [c]						
cis-SnI_4L_2	158.36	–	–	–	2.813(2)	I–Sn–I
	163.42	–	–	–	2.782(2)	I–Sn–O
L = bipy						
cis-$SnHaI_4L$	153.68	–	–	–	2.816(2)	I–Sn–I
	169.29	–	–	–	2.788(2)	I–Sn–N
L = DMSO						
cis-SnI_4L_2	150.65	–	–	–	–	I–Sn–I
	166.55	–	–	–	–	I–Sn–O
cis-$Et_2SnI_2L_2$	70.83	119.30	409.07	39.1	2.941(1)	I–Sn–O
	79.96	156.34	523.00	13.3	2.982(1)	I–Sn–O
$Ph_2SnI_2L_2$	103.17	192.00	647.32	24.3	–	–
	107.02	212.04	707.80	8.6	–	–
L = py						
trans-SnI_4L_2	162.66	–	–	–	–	I–Sn–I
$Et_2SnI_2L_2$	80.92	149.36	504.35	25.7	–	I–Sn–I
	82.01	162.38	542.13	8.8	–	I–Sn–I
$Ph_2SnI_2L_2$	98.11	187.68	630.03	18.9	–	I–Sn–I
L = DPSO						
cis-SnI_4L_2	154.41	305.00	1018.70	9.8	2.806(1)	I–Sn–I
	163.72	–	–	–	2.781(1)	–
	164.58	–	–	–	2.776(1)	–
	167.22	–	–	–	2.773(1)	–
cis-$EtSnI_3L_2$	130.50	–	–	–	2.869(1)	I–Sn–I
	136.50	268.00	895.10	12.4	2.840(1)	I–Sn–I
					2.821(1)	I–Sn–O

Note. Resonance frequencies of chemically equivalent iodine atoms are averaged over crystallographically inequivalent positions. The values expected by analogy to those measured for the related compounds are given in braces.
[a] Calculated. [b] The unit cell comprises two crystalographically independent molecules of the adduct. [c] Triphenylphosphine oxide.

As is seen from Tables 3 and 4, the prevailing effect of substitution is, in agreement with the earlier conclusions,[17] weakening of the *cis*-Sn–Hal bonds relative to the substituent R as compared to the Sn–Cl bonds in the corresponding non-substituted complexes (adducts). The elongation of the Sn–Hal bond by 0.1 Å is accompanied by an increase in the effective negative charge on the chlorine, bromine and iodine atoms by *ca.* 0.08, 0.1 (see Ref. 18) and 0.12 e (see Ref. 12), respectively. It is noteworthy that according to the X-ray data the elongation of the *cis*-Sn–Hal bond relative to the substituent R is the same for all the monoalkyl-substituted adducts of any halogen element, amounting approximately to 0.1 Å. The similar bond elongation is accompanied by an increment of the negative charge on the corresponding halogen atom, which points to an increase in *cis*-weakening due to the alkyl group in the order Cl < Br < I.[12, 18]

Phenyl substituents also weaken the appropriate Sn–Hal bonds, although to a lesser extent. The effective charges born by the iodine atoms in dialkyl- and diphenyl-substituted adducts $R_2SnI_2L_2$ were estimated [12] to differ, on average, by 0.08 e. In adducts of mono-substituted tin halides, both *cis*-weakening and *trans*-strengthening are also more pronounced in alkyl-substituted adducts than in phenyl analogues (Tables 1 and 3). Variations of the effective charges on the halogen atoms in *cis*- and *trans*-positions to the substituent R as well as their valence p_π orbital occupancies resulting from substitution can clearly be compared on a quantitative scale. As follows from comparison of the absolute magnitudes of $\Delta\rho$ (Table 3), a negative charge increment on the halogen atoms, *i.e.*, the effect of *cis*-weakening of the Sn–Hal bond as a result of substitution, is 2–3 times as strong as that of *trans*-strengthening. Comparison of the corresponding

Table 3. Changes in the Sn – Hal bond characteristics in the adducts of tin tetrahalides as a result of substitution $SnHal_4L_2 \rightarrow RSnHal_3L_2$.

Compound	Np_σ	ΔNp_π	$-\rho$ /e	$\Delta\rho$ (%)	Δd (%)	Assignment
$(NMe_4)_2SnCl_6$	1.696	0.0 [a]	0.696	–	–	Cl – Sn – Cl
$(NMe_4)_2EtSnCl_5$	1.670	0.0 [a]	0.670	−3.7	−0.7	Cl – Sn – Et
	1.768	0.015	0.753	+8.2	+3.8	Cl – Sn – Cl
$(NMe_4)_2SnBr_6$	1.642	0.0 [a]	0.642	–	–	Br – Sn – Br
$(NMe_4)_2EtSnBr_5$	1.585	0.0 [a]	0.585	−8.9	−1.5	Br – Sn – Et
	1.733	0.017	0.716	+11.5	+3.6	Br – Sn – Br
$(MeNH_3)_2SnCl_6$	1.712	0.0 [a]	0.712	–	–	Cl – Sn – Cl
$(MeNH_3)_2EtSnCl_5$	1.684	0.012	0.672	−5.6	+0.4	Cl – Sn – Et
	1.772	0.017	0.755	–	–	Cl – Sn – Cl
	1.780	0.020	0.760	+8.0	+4.3	Cl – Sn – Cl
	1.794	0.020	0.774	???	(åÆ.)	Cl – Sn – Cl
	1.809	0.021	0.788	–	–	Cl – Sn – Cl
$(PyH)_2SnCl_6$	1.698	0.0 [a]	0.698	–	–	Cl – Sn – Cl
$(PyH)_2EtSnCl_5$	1.673	0.0 [a]	0.673	−3.6	−1.2	Cl – Sn – Et
	1.785	0.019	0.766	+9.7	+2.8	Cl – Sn – Cl
L = TMU						
$SnCl_4L_2$	1.659	0.017	0.642	–	–	Cl – Sn – Cl
$EtSnCl_3L_2$	1.645	> 0.003	< 0.642	< 0.0	−0.7	Cl – Sn – Et
	1.748	0.012	0.736	+14.6	+4.2	Cl – Sn – Cl
L = DMSO						
$SnCl_4L_2$	1.662	0.007	0.655	–	–	Cl – Sn – Cl
	1.676	0.029	0.647	–	–	Cl – Sn – O
$EtSnCl_3L_2$	1.688	0.006	0.682	+4.1	+0.7	Cl – Sn – Et
	1.743	0.023	0.720	+11.2	+2.7	Cl – Sn – O
L = HMPT						
$SnCl_4L_2$	1.663	0.023	0.640	–	–	Cl – Sn – Cl
$EtSnCl_3L_2$	1.630	0.097	0.620 [b]	−3.2	−0.4	Cl – Sn – Et
					+4.3	Cl – Sn – Cl
$PhSnCl_3L_2$	1.655	< 0.015	< 0.640	< 0.0	–	Cl – Sn – Ph
	1.735	0.019	0.716	+11.9	–	Cl – Sn – Cl
$SnBr_4L_2$	1.589	0.028	0.561	–	–	Br – Sn – Br
$BuSnBr_3L_2$	1.579	> 0.018	< 0.561	< 0.0	−0.8	Br – Sn – Bu
	1.698	0.020	0.678	+20.8	+3.2	Br – Sn – Br
L = THF						
$SnCl_4L_2$	1.639	0.031	0.607	–	–	Cl – Sn – Cl
$MeSnCl_3L_2$	1.624	> 0.017	< 0.607	< 0.0	–	Cl – Sn – Me
	1.707	0.025	0.682	+12.3	–	Cl – Sn – Cl
$SnBr_4L_2$	1.571	0.037	0.534	–	–	Br – Sn – Br
$MeSnBr_3L_2$	1.552	> 0.018	< 0.534	< 0.0	–	Br – Sn – Me
	1.661	0.029	0.632	+18.3	–	Br – Sn – Br

[a] In the absence of the experimental data, it was assumed that $\eta = 0$; from symmetry considerations, the real η-value should not exceed 5% – 10%. [b] At $\eta = 4\%$.

values for ΔNp_π shows that the equatorial π-bonds in monoalkyl-substituted adducts remain virtually undisturbed by *cis*-weakening, whereas *trans*-strengthening seems to involve both σ- and π-bonds. In most of the $RSnHal_3L_2$ compounds, *trans*-strengthening of the Sn – Hal bond occurs only if η is non-zero, hence revealing disturbance of the halogen π-system. In chlorine-containing adducts, the η-values, at which *trans*-strengthening takes place, show the tendency to an increase as the donating power of either substituent R (provided the ligand L remains the same) or ligand L (provided the substituent R remains the same) decreases. Thus, *trans*-strengthening in the adduct $PhSnCl_3(HMPT)_2$ can only be observed when the η-value for the appropriate chlorine atom reaches 6.7%, whereas in its ethyl analogue $EtSnCl_3(HMPT)_2$, it is observed at $\eta = 0$ and reaches 3% at $\eta = 4\%$. However, *trans*-strengthening in the adduct

Table 4. Changes in the Sn – Hal bond characteristics in the adducts of tin tetrahalides as a result of substitution $SnHal_4L_2 \rightarrow R_2SnHal_2L_2$.

Compound	Np_σ	ΔNp_π	$-\rho$ /e	$\Delta\rho$ (%)	Δd (%)	Assignment
L = HMPT						
$SnCl_4L_2$	1.663	0.023	0.640			Cl – Sn – Cl
$Me_2SnCl_2L_2$	1.822	0.012	0.810	+26.6	+7.6	Cl – Sn – Cl
SnI_4L_2	1.543	0.006	0.537			I – Sn – I
	1.514	0.019	0.495			I – Sn – O
$Et_2SnI_2L_2$	1.791	0.009	0.782	+51.5	+7.8 [a]	I – Sn – I
$Ph_2SnI_2L_2$(I)	1.754	0.059	0.695	+34.7	+5.7 [a]	I – Sn – I
(II)	1.750	0.060	0.689	+33.5	+5.0 [a]	I – Sn – I
$SnBr_4L_2$	1.589	0.028	0.561			Br – Sn – Br
$Me_2SnBr_2L_2$	1.805	0.014	0.791	+41.0	+7.4	Br – Sn – Br
L = TMU						
SnI_4L_2	1.540	0.006	0.534			I – Sn – I
	1.512	0.019	0.493			I – Sn – O
$SnBr_4L_2$	1.604	0.018	0.586			Br – Sn – Br
$Et_2SnBr_2L_2$	1.759	0.011	0.748	+27.6		Br – Sn – Br
L = DMF						
$SnCl_4L_2$	1.670	0.012	0.658			Cl – Sn – Cl
$Me_2SnCl_2L_2$	1.793	0.008	0.785	+19.3		Cl – Sn – O
L = DMSO						
$Et_2SnI_2L_2$	1.798	0.046	0.752	+52.5 [b]	+5.0 [c]	I – Sn – O
	1.762	0.020	0.742	+50.5 [b]	+6.4 [c]	I – Sn – O
$Ph_2SnI_2L_2$	1.695	0.046	0.649	+31.6 [b]		–
	1.682	0.018	0.665	+34.9 [b]		–
$SnBr_4L_2$	1.629	0.007	0.622			Br – Sn – Br
	1.586	0.037	0.549			Br – Sn – O
$Me_2SnBr_2L_2$	1.807	0.017	0.790	+35.0	+7.7 [d]	Br – Sn – Br
$SnCl_4L_2$	1.662	0.007	0.655			Cl – Sn – Cl
	1.676	0.029	0.647			Cl – Sn – O
$Me_2SnCl_2L_2$	1.802	0.017	0.785	+21.3	+5.0	Cl – Sn – O
L = bipy						
$SnBr_4L$	1.630	0.004	0.630			Br – Sn – Br
	1.577	0.041	0.536			Br – Sn – N
Bu_2SnBr_2L	1.757	0.024	0.733	+36.7	+6.8	Br – Sn – N
L = THF						
$SnBr_4L_2$	1.571	0.037	0.534			Br – Sn – Br
$Me_2SnBr_2L_2$	1.679	0.028	0.651	+21.9		Br – Sn – Br
L = py						
$Et_2SnI_2L_2$	1.761	0.038	0.723			I – Sn – I
	1.757	0.014	0.742			I – Sn – I
$Ph_2SnI_2L_2$	1.708	0.035	0.673			I – Sn – I
$SnBr_4L_2$	1.601	0.038	0.563			Br – Sn – Br
$Et_2SnBr_2L_2$	1.790	0.020	0.770	+36.8		Br – Sn – Br
$Me_2SnBr_2L_2$	1.786	0.020	0.766	+36.1		Br – Sn – Br

[a] With respect to $SnI_4(Ph_3PO)_2$. [b] With respect to $SnI_4[(Me_2N)_2CO]_2$. [c] With respect to SnI_4(bipy). [d] With respect to $SnBr_4(Ph_2SO)_2$.[23]

$EtSnCl_3(THF)_2$ is only possible at $\eta > 7\%$. Although the contribution of the π-system to chemical bonding in tin adducts is small, the above tendency is clearly seen from the NQR data.

As a whole, the electronic effects of substitution in the adducts with known structure were found to correlate to their structural manifestations, although in the adducts of mono-substituted tin chlorides, a shortening of the Sn – Hal bond in the *trans*-position to the substituent R was small and comparable with the standard deviation values. In $(MeNH_3)_2EtSnCl_5$, no shortening of the *trans*-bond Sn – Hal compared to the parent unsubstituted complex was found by X-ray analysis,[19] whereas the absolute value of

the effective charge on the *trans*-ligand decreased by more than 5%, the appropriate frequency shift exceeding 1 MHz. The frequency shifts at the chlorine atoms in *trans*-positions to the substituent observed in the NQR spectra of all compounds studied notably exceeded the errors of measurement, so that the effect of *trans*-strengthening was readily revealed in terms of a decrease in the effective charge on the corresponding chlorine atom. The NQR parameters are more sensitive to the influence of substituents than the interatomic distances (Tables 3 and 4); this is however not unexpected, considering that the substituent influence is governed by the electronic effects, whereas the NQR parameters directly reflect the electron density variations on the atom under study.

It is worthwhile to compare redistribution of the electron density in adducts of mono-substituted tin halides with different mutual arrangement of the ligands L. For instance, in Tables 1 and 3, the data are summarised for the adducts *cis*-$EtSnCl_3(DMSO)_2$ (**1**) and *trans*-$PhSnCl_3(HMPT)_2$ (**2**), whose strong donor ligands L are competitive in donating power with the substituents R. One can see that *cis*-weakening of the Sn—Hal bonds in the adduct **1**, where the ligands DMSO are in *cis*-position to each other, is less pronounced than that in the ethyl-substituted adducts with weaker donor ligands L. Moreover, in agreement with X-ray data, *trans*-strengthening of the Sn—Hal bond in **1** gives way to *trans*-weakening. By contrast, *trans*-strengthening of the Sn—Hal bond exists in the molecule **2** with *trans*-position of the HMPT ligands relative to each other, as follows from the NQR frequency shift, and *cis*-weakening in this adduct is stronger than in **1**, although the phenyl group is a weaker 'influencing' substituent than the ethyl group.

Introduction of the second substituent R to give an adduct $R_2SnHal_2L_2$ increases the *cis*-lengthening (weakening) of the Sn—Hal bond in an approximately additive manner. As a result, in the adducts of dialkyltin dichloride, dibromide and diiodide the effects exceed 25%, 40% and 50%, respectively, the appropriate Sn—Hal bond elongation being ~ 0.2 Å. Whereas the *cis*-weakening effect of the phenyl substituents is less than that due to the ethyl groups, the effects due to different alkyl groups are approximately the same, as one can see from the data for $Me_2SnBr_2(py)_2$, $Et_2SnBr_2(py)_2$ and $Bu_2SnBr_2(bipy)_2$ (Table 4). It thus follows that the variations from 22% to 41% in *cis*-weakening of the Sn—Br bonds in the adducts of dialkyldibromostannates are caused by different contributions of the ligands L into the combined effect of *cis*-weakening: THF < TMU < DMSO $\simeq$ py $\simeq$ bipy < HMPT.

In studies of adducts of dialkyl(diphenyl)diiodostannates it was found [12, 25] that the elongation of the Sn—I bond with respect to that in the parent adduct was accompanied by a dramatic increase in η at the iodine sites. Such an increase was observed in five of six adducts studied by NQR (Table 5), which implies that the iodine valence $5p_\pi$ orbitals were notably disturbed as a result of the substitution, which gives rise to an essential increase in the occupancy difference $\Delta Np_\pi = Np_x - Np_y$. NQR spectroscopic and X-ray diffraction data for the two adducts were correlated in order to understand the reason for this disturbance.[26]

As one can see from Table 5, the largest increase in η upon replacement of two iodine atoms by the groups R is observed in the adducts $Ph_2SnI_2(HMPT)_2$ (**3**) and $Et_2SnI_2(DMSO)_2$ (**4**). The ^{127}I NQR spectrum of the adduct **3** consists of two sets of lines corresponding to two crystallographically inequivalent iodine sites having close spectroscopic characteristics. The introduction of the phenyl groups resulted in the elongation of the Sn—I bonds by 0.165 Å on average with respect to those in the nonsubstituted adduct $SnI_4(TPPO)_2$ whose structure is known and spectroscopic characteristics are similar to those in the yet as structurally unstudied adducts $SnI_4(HMPT)_2$ and $SnI_4(TMU)_2$ (Table 2). As the comparison of the iodine valence orbital occupancies in substituted and nonsubstituted adducts shows (Table 5), the substitution results in an increase in the iodine valence $5p_\sigma$ orbital occupancies (Np_z), which is a natural consequence of the *cis*-weakening of the Sn—I bonds. The latter is however accompanied by a notable increase in the iodine valence $5p_\pi$ orbital occupancy difference ($\Delta Np_\pi = Np_x - Np_y$) from 0.019 in nonsubstituted $SnI_4(TMU)_2$ to 0.06 in the adduct **3**.

The obvious suggestion accounting for such an increase in η in compound **3** is that secondary non-valence intra- or intermolecular contacts exist in this compound that involve the iodine atoms. The results of the X-ray study do not, however, support this suggestion: no secondary contacts were found in the structure of **3**.[26]

In the crystals of the adduct **4**, two crystallographically inequivalent iodine positions (characterised by substantially different spectroscopic parameters) were identified by NQR. According to the X-ray diffraction data, the coordination polyhedron around tin is an octahedron with *trans* ethyl groups and *cis* DMSO molecules (Fig. 1 *a*). Both DMSO molecules occupy disordered positions, so that the sulfur atom of one DMSO molecule occupies the positions at the opposite sides of the O(1)C(5)C(6) plane, whereas in the other molecule, both sulfur and oxygen atoms are sited at disordered positions. Table 6 lists the bond lengths and angles for the prevailing configuration of the

Table 5. ^{127}I NQR spectroscopic parameters for adducts $R_2SnI_2L_2$ and SnI_4L_2 at 77 K and the Sn—I bond characteristics.[26]

Compound	e^2Qq_{zz}/h /MHz	a/e	η (%)	Np_z	$\Delta Np_\pi = Np_x - Np_y$ ($Np_x = 2$)	$-\rho$ /e	d /Å
cis-$Et_2SnI_2(DMSO)_2$	409.1		39.1	1.798	0.046	0.752	2.941
	523.0		13.3	1.762	0.020	0.742	2.982
						0.690 [a]	
$Ph_2SnI_2(DMSO)_2$	647.3		24.3	1.695	0.046	0.649	
	707.8		8.6	1.682	0.018	0.665	
trans-$Et_2SnI_2(HMPT)_2$	467.9		6.5	1.791	0.009	0.782	3.016
trans-$Ph_2SnI_2(HMPT)_2$(I)	495.2		41.2	1.754	0.059	0.695	2.957
(II)	504.1		41.2	1.750	0.060	0.689	2.938
cis-$SnI_4(TMU)_2$	1048.0	a	1.9	1.540	0.006	0.534	
	1095.3	e	6.0	1.512	0.019	0.493	
cis-$SnI_4 \cdot bipy$		a					2.816
		e					2.788
$Et_2SnI_2(py)_2$	504.35		25.7	1.761	0.038	0.723	
	542.1		8.8	1.757	0.014	0.742	
$Ph_2SnI_2(py)_2$	630.03		18.9	1.708	0.035	0.673	

Note. Here and in tables below: a is axial, e is equatorial halogen atoms; for the remaining notations see Table 3. [a] See text.

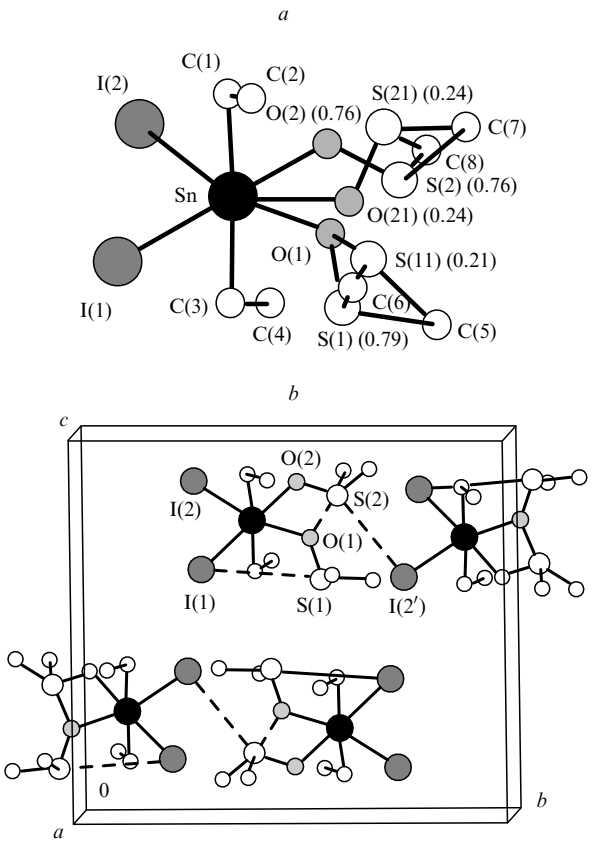


Figure 1. Structure of the adduct $Et_2SnI_2(DMSO)_2$;[26]
(*a*) molecular structure of $Et_2SnI_2(DMSO)_2$, illustrating disorder in the DMSO ligands; occupancies of the atomic positions are given in parentheses;
(*b*) crystal structure of the adduct showing non-valence contacts (dotted lines); only prevailing conformation retained.

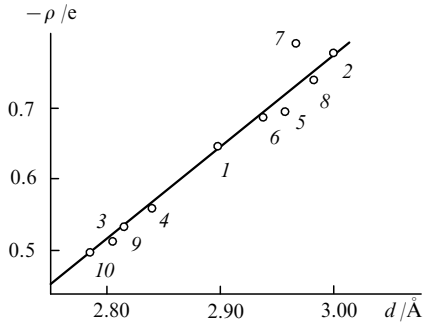


Figure 2. Correlation between the effective charges on the iodine atom ($-\rho$) and interatomic Sn−I distances (*d*);[12] (*1*) $EtSnI_3(HMPT)_2$, (*2*) $Et_2SnI_2(HMPT)_2$, (*3*) $SnI_4(Ph_2SO)_2$, (*4*) $EtSnI_3(Ph_2SO)_2$, (*5*, *6*) $Ph_2SnI_2(HMPT)_2$, (*7*, *8*) $Et_2SnI_2(DMSO)_2$, (*9*, *10*) $SnI_4(TMU)_2$.

adduct molecule. In the strucutre of the adduct **4**, the intramolecular [S(2)···O(1) = 3.06 Å, S(1)···I(1) = 4.11 Å], and intermolecular [S(2)···I(2′) = 3.79 Å] contacts (Fig. 1 *b*) were found, hence revealing at least one of the reasons for the increase in the value of η (39.1%) in this adduct.

On the plot giving the effective charge on the iodine atom as a function of the respective Sn – I bond lengths (Fig. 2), deviation of the point *7*, corresponding to the I(1) site in the adduct **4** from the correlation line is a maximum. Note that the effective charges were evaluated assuming that the occupancy of one of the iodine $5p_\pi$ orbitals (Np_x) was equal to 2.[26] As Fig. 2 shows, such an assumption results in a good correlation between $-\rho$ and the Sn−I bond lengths for all the points in the adducts discussed except that for the I(1) atom in compound **4**. The effective charge on this atom (for the same values of experimentally measured QCC and η) for the point *7* to fit the correlation line should be equal to −0.69 e (Table 5), which gives the following iodine valence orbital occupancies: $Np_z = 1.778$, $Np_x = 1.979$ and $Np_y = 1.933$. Thus, the deviation of the point *7* from the correlation serves as indirect evidence that the assumption $Np_x = 2$ underestimates the Sn−I π-bonding character for the I(1) atom involved in secondary contact to sulfur. This contact is associated with the transfer of ~ 0.042 e from the iodine valence $5p_\pi$ orbitals.

The probable reason for the increased η-value (39.1%) in the adduct **3**, where no shortened contacts were found, was sought in the analysis of contributions of the iodine valence 5*p* orbital occupancies into the measured value of η. It was shown that despite similar values of the asymmetry parameters at the iodine sites in **3** and the I(1) site in **4** the difference $\Delta Np_\pi = Np_x - Np_y$ in the latter adduct is less than in the former one. As has been mentioned above, the alkyl substituents weaken the respective Sn−I bonds to a greater extent than the phenyl groups, thus producing higher occupancy of the iodine $5p_\sigma$ orbitals. A sharp increase in the experimentally measured η-value occurs, at the fixed $\Delta Np_\pi = Np_x - Np_y$ difference, as the σ-electron density at the iodine atom (Np_z) increases (Fig. 3), *i.e.*, the enhanced *cis*-weakening of the Sn−I bond due to substitution results, at a given ΔNp_π difference, in an increase in the asymmetry parameter η caused by the increased contribution to the latter of the iodine valence $5p_\sigma$ orbitals. Indeed, the closely similar values of η in **3** and at the I(1) site in **4** are associated with a relatively smaller iodine $5p_\pi$ orbital occupancy difference in the latter adduct, since the alkyl substituents favour an increase in σ-electron density on the iodine atoms to a larger extent than the phenyl groups do.

Thus, an increase in the η-value in the adduct **4** (Table 5) is caused by the combined contribution of the iodine valence $5p_\sigma$ orbitals, whose occupancy increases upon substitution, and the shortened I···S contacts responsible for an increase in ΔNp_π. As to the increased ΔNp_π difference in the adduct **3**, this is most

Table 6. Bond lengths (*d*) and bond angles (α) in the adduct **4**.[26]

Bond	*d* /Å	Angle	α /deg	Angle	α /deg
Sn−I(1)	2.982(1)	I(1)−Sn−I(2)	100.40(4)	(1)−Sn−O(2)	80.2(3)
Sn−I(2)	2.941(1)	I(1)−Sn−O(1)	95.4(2)	O(1)−Sn−C(1)	88.9(3)
Sn−O(1)	2.220(6)	I(1)−Sn−O(2)	173.9(2)	O(1)−Sn−C(3)	92.0(4)
Sn−O(2)	2.253(8)	I(1)−Sn−C(1)	90.7(3)	O(2)−Sn−C(1)	85.0(4)
Sn−O(21)	2.16(2)	I(1)−Sn−C(3)	84.6(3)	O(2)−Sn−C(3)	99.7(4)
Sn−C(1)	2.164(10)	I(2)−Sn−O(1)	163.9(2)	C(1)−Sn−C(3)	175.3(4)
Sn−C(2)	2.174(10)	I(2)−Sn−O(2)	83.8(2)		
		I(2)−Sn−C(1)	87.7(3)		
		I(2)−Sn−C(3)	92.7(3)		

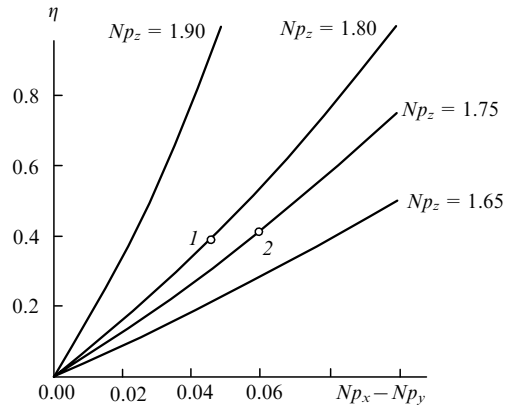


Figure 3. Measured value of the EFG asymmetry parameter (η) at the iodine atom as a function of its valence π-orbital occupancy difference ($Np_x - Np_y$) for various σ-orbital occupancies (Np_z);[26]
(*1*) is the point corresponding to the point (*7*) and (*2*), to the points (*5*) and (*6*) on the plot of Fig. 2.

probably associated with the interaction of the iodine π-system with those of the phenyl rings. This suggestion is supported by the fact that in the $Et_2SnI_2(HMPT)_2$ adduct, which is a dialkyl analogue of **3** comprising no cyclic fragments in the ligands and substituents, the alkyl groups did not give rise to an increase in ΔNp_π and consequently in the EFG asymmetry parameter η. However, replacement of the ethyl by phenyl substituents affected dramatically the asymmetry parameter η, although no proper structural manifestations could be registered by X-ray diffraction. This is one of a few examples illustrating a possibility to detect, using NQR, the electronic effects, whose structural manifestations lie below the sensitivity of X-ray experiments. Yet another example was given above in the effects of *trans*-strengthening. The accuracy of their determination in chlorides is, as a rule, comparable to the standard deviations, whereas the corresponding variations of the NQR parameters notably exceed the errors of measurement. It is however to be noted that there are many other systems in which π–π interactions were clearly revealed by X-ray studies. For instance, the π–π interactions between the iodine atoms and phenyl rings were earlier found by X-ray in several imidazopyridinium salts.[27]

The NQR and X-ray data yield complementary pieces of valuable information. A correlation between them on a quantitative scale contributes to the further progress in understanding the electronic effects of substitution in adducts and complexes of tin(IV) halides, augmenting the current view by information on relative importance of the σ- and π-electron systems in electron density redistribution.

III. Electronic characteristics of M—Hal bonds in hexa- and pentacoordinate adducts of tin(IV) tetrachlorides; similarities and differences

In this section, the M—Hal bond reorganisation in adducts of tin tetrahalides resulting from the change in the central metal coordination number is discussed. The data on electron density redistribution due to spatial rearrangement of adducts, especially those of silicon and germanium, are scanty. The literature on ^{35}Cl NQR studies of hexa- and pentacoordinate adducts of tin tetrachloride is more extensive. However, *cis*–*trans* isomerism of hexacoordinate tin(IV) adducts complicated comparative studies of the bond electronic characteristics in these compounds, because no reliable spectroscopic criteria of either isomerism or assignment of the ^{35}Cl NQR frequencies in *cis*-isomers to axial–equatorial chlorine atoms were available.

NQR studies of pseudooctahedral adducts $SnCl_4L_2$ have received major attention. The subjects of investigations were the structures of the compounds,[28—34] charge distribution over acceptor molecules,[33–39] relation of the ligand donating power to the strength of the produced adducts judging from spectroscopic data[40] and identification of isomers based on their NQR spectra.[40–42] A bibliography on these problems covering the period since 1980 to the beginning of the 90's may be found in a review.[43]

Studies on isomerism of pseudooctahedral adducts of tin tetrachloride show[40] that the frequency splitting in the NQR spectra of *cis*-isomers (*i.e.*, the difference between the frequencies of equatorial and axial chlorine atoms) cannot serve as a reliable criterion of isomerism, because its magnitude decreases as the donating power of ligands L increases. For strong adducts, this prevents the spectroscopic identification of *cis*- and *trans*-isomers. An unambiguous identification of isomers is further complicated where the NQR spectra of *trans*-isomers are affected by crystal-field effects, which enhance the frequency splitting, and mask their difference from the spectra of *cis*-isomers. Temperature dependences of the NQR frequencies of equatorial and axial chlorine atoms do not always clarify the situation.[41,42] For the isomers with established *cis*-configuration, the assignment of resonance frequencies to equatorial–axial atoms is also ambiguous. According to the X-ray data available on a relatively few *cis*-$SnCl_4L_2$ adducts, the number of adducts whose axial Sn—Cl bond distances are shorter than the equatorial ones is approximately the same as that whose axial Sn—Cl bond distances exceed equatorial. The identification of a large number of $SnCl_4L_2$ isomers was made[40] assuming that in NQR spectra of both *cis*- and *trans*-isomers the ^{35}Cl frequencies of the atoms making a linear Cl—Sn—Cl fragment are close to each other if the donating powers of ligands L are similar. As a result, the higher ^{35}Cl frequencies in the NQR spectra of *cis*-isomers were erroneously assigned to linear Cl—Sn—L fragments.

Thus, a considerable body of experimental data showed that neither frequency splittings and line multiplicity nor temperature dependence of the NQR frequencies can be recognised as reliable criteria for identification of isomers. However, the symmetry considerations suggest that the EFG asymmetry parameters at axial–equatorial chlorine sites may possibly serve as such criteria, although the values of η and QCC cannot be simultaneously found, without additional experiments, from only one transition frequency for nuclei with $I = 3/2$ having two degenerate quadrupole levels. Conventional Zeeman NQR experiments with single crystals are however complicated and tedious, serious limiting factors being duration of experiments and problems of growing large single crystals of tin tetrachloride adducts, most of which are hygroscopic.

Attempts at experimental determination of η at the chlorine atoms in powder samples were undertaken[8] using a modified approach[3] based on Fourier analysis of slow beats of the spin-echo envelope in an external magnetic field. The experiment was run according to the scheme: NQR spectrometer ⟷ programmer and digitiser ⟶ box-car integrator ⟶ computer. The programmer and digitiser were adapted to the tube levels of NQR signals. Instead of the conventional Fourier transform used in NMR spectroscopy, the data processing involved expansion of a signal to harmonics followed by numerical integration for determining the expansion coefficients. As a result, the accuracy of the analysis increased, whereas its duration remained shorter than the time of signal accumulation. The Fourier transform programme was used which yielded a graphic representation of both the accumulated spectrum of slow beats and its expansion into harmonics. This easy-to-grasp form of representation of the results enabled the authors to monitor the data processing checking the operation for errors. The accuracy of η measurements performed by this procedure even on weak ^{35}Cl signals was fairly high.

In subsequent experiments, the results of determination of η in a number of *cis*- and *trans*-isomers of $SnCl_4L_2$ adducts con-

firmed [11] that the EFG asymmetry parameters can actually be used for identification of isomers (Tables 7 and 8). Thus the magnitudes of η on axial chlorine atoms in *cis*-isomers appeared to be zero unless lattice contributions raised its value by several percent. On equatorial Cl atoms of both isomers, the η-values were usually noticeably higher, varying around 10% in the majority of the compounds.

For comparison, the results of Zeeman analysis of single crystals at 297 K, 293 K and 235 K available for several hexacoordinate adducts, are also listed in Tables 7 and 8.[44–46] They are in reasonable agreement with those obtained with powder samples: the magnitudes of orbital occupancies and effective charges on the chlorine atoms derived from both experiments are consistent with each other. The approach for measuring η in powder samples simplified the experiment and markedly cut its time. The important benefit to the user consists in avoiding a tedious long-term procedure of growing large single crystals required for the NQR Zeeman experiments.

The determination of the total set of NQR spectroscopic parameters (the transition resonance frequencies ν, quadrupole coupling constant QCC and EFG asymmetry parameter η) for a number of adducts, which became possible due to the use of powder samples, revealed the regularities of electron density redistribution between axial–equatorial bonds (Fig. 4) which thereafter allowed identification of *cis*- and *trans*-isomers of some adducts that had not been studied structurally based only on the NQR frequency measurements.[10]

The ^{35}Cl NQR frequencies assigned to the axial chlorine atoms in the spectra of all the *cis*-isomers examined [10] appeared to be higher and the σ-electron density on the respective Cl atoms lower than those on the equatorial chlorine atoms. The frequency ranges assigned to axial and equatorial Cl atoms did not virtually overlap, so that the corresponding frequencies in the spectra of *cis*-isomers were found in the intervals (MHz) $17.5 < \nu_e < 19.8 < \nu_a < 22.0$, whereas the region covered by the ^{35}Cl frequencies in the spectra of *trans*-isomers was slightly shifted downwards: $17.2 < \nu_e < 19.4$. The effective charges on the Cl atoms were practically insensitive to the kind of isomerism of the adduct, their magnitudes being approximately the same on both axial and equatorial chlorine sites and in both types of isomers (Tables 7 and 8).

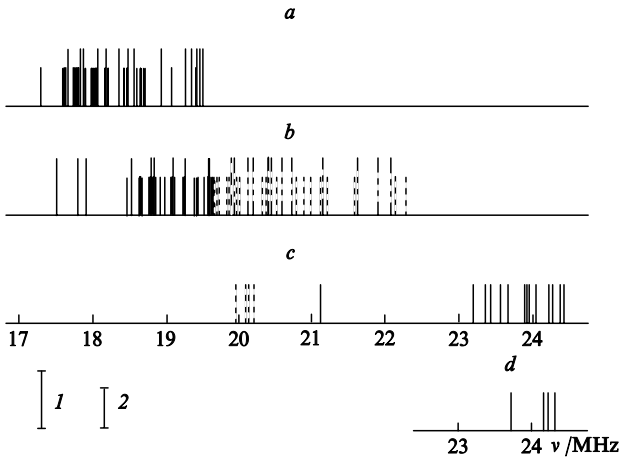


Figure 4. The diagrams of ^{35}Cl NQR spectra of pseudooctahedral adducts: *trans*-$SnCl_4L_2$ (*a*), *cis*-$SnCl_4L_2$ (*b*), trigonal-bipyramidal adducts $SnCl_4L$ (*c*) and parent tin tetrachloride (*d*). The ^{35}Cl frequencies with measured (*1*) and unknown (*2*) magnitudes of η; the dotted bars are axial, the solid bars are equatorial chlorine positions.

The results of the study cited (Ref. 10) show that the *cis*-isomer of adduct $SnCl_4L_2$ can be identified by the presence in its NQR spectrum of the ^{35}Cl signals at frequencies above 19.8 MHz, which should be assigned to the axial Cl–Sn–Cl fragments. More than 80% of *trans*-isomers examined so far gave NQR spectra with the ^{35}Cl average frequencies below 18.3 MHz, while 80% of *cis*-isomers had them above 19.3 MHz. It is to be emphasised however that the above regularities in electron density distribution are only valid for the molecular adducts, whose chlorine atoms are bonded only to the central atom and are not involved in secondary inter- or intramolecular interactions.

Table 7. ^{35}Cl NQR spectroscopic parameters for *trans*-isomers of hexacoordinate adducts of tin tetrachloride at 77 K and the M–Cl bond characteristics.[9]

L	ν /MHz	η (%)	e^2Qq_{zz}/h /MHz	Np_σ	ΔNp_π	$-\rho$ /e	$\lvert\sum\rho\rvert$ /e
Diox	19.41	6.1 ± 1.5	38.80	1.639	0.014	0.625	2.500
DMF	17.77	5.7 ± 1.0	35.52	1.670	0.012	0.658	2.632
TMU	18.36	8.4 ± 0.5	36.68	1.656	0.019	0.637	2.568
	18.16	6.7 ± 1.9	36.29	1.662	0.015	0.647	
THF	19.39	15.8 ± 3.0	38.62	1.628	0.037	0.591	2.426
	19.25	13.4 ± 1.1	38.38	1.634	0.031	0.603	
	18.91	12.2 ± 1.1	37.73	1.641	0.028	0.613	
	18.54	12.8 ± 1.2	36.98	1.648	0.029	0.619	
DEE	19.44	13.6 ± 3.1	38.76	1.630	0.032	0.598	2.390
	19.47	13.6 ± 3.1	38.82	1.629	0.032	0.597	
	19.341 [a]	11.4	38.600				
	19.440 [a]	11.6	38.793				
HMPT	17.77	10.8 ± 2.1	35.47	1.665	0.023	0.642	2.558
	18.04	10.4 ± 1.4	36.02	1.660	0.023	0.637	
py	17.76	15.4 ± 2.6	35.38	1.660	0.033	0.627	2.512
	17.64	15.4 ± 2.6	35.14	1.662	0.033	0.629	
DBS	18.48	15.2 ± 4.1	36.81	1.647	0.034	0.613	2.464
	18.18	15.5 ± 3.4	36.22	1.653	0.034	0.619	
acac	19.94(2)	5.5 ± 0.9	39.86	1.630	0.013	0.617	2.493
	19.48	5.2 ± 1.0	38.94	1.639	0.012	0.627	
	18.28	10.5 ± 2.1	36.49	1.655	0.023	0.632	

Note. Diox is dioxane, DEE is diethyl ether, DBS is dibenzyl sulfide, acac is acetylacetonate; $\lvert\sum\rho\rvert$ is the total effective charge on the chlorine atoms in the adduct. [a] The results of Zeeman analysis of a single crystal at 235 K.[44]

Table 8. ^{35}Cl NQR spectroscopic parameters for *cis*-isomers of hexacoordinate adducts of tin tetrachloride at 77 K and the M–Cl bond characteristics.[9]

L	a/e	ν /MHz	η (%)	e^2Qq_{zz}/h /MHz	Np_σ	ΔNp_π	$-\rho$ /e	$\lvert\sum\rho\rvert$ /e
$POCl_3$	a	21.13	2.3 ± 0.5	42.26	1.612	0.006	0.606	2.425
	e	19.79	11.1 ± 2.0	39.50	1.627	0.027	0.600	
	e	19.03	11.7 ± 2.4	37.97	1.640	0.027	0.613	
	a [a]	20.924	1.2 ± 0.1	41.847	1.617	0.003	0.614	2.475
	e [a]	19.093	8.8 ± 0.4	38.134	1.642	0.020	0.622	
	e [a]	18.852	9.2 ± 0.1	37.651	1.646	0.021	0.625	
$P_2O_3Cl_4$	a	22.05	4.8 ± 1.6	44.08	1.592	0.013	0.579	2.351
	a	21.87	5.6 ± 1.6	43.72	1.594	0.015	0.579	
	e	19.77	12.8 ± 3.0	39.43	1.625	0.031	0.594	
	e	18.49	19.6 ± 2.1	36.74	1.643	0.044	0.599	
Me_2O [b]	a	20.287	2.7	40.569	1.627	0.007	0.620	2.520
	e	18.807	4.9	37.600	1.651	0.011	0.640	
MeCN	a	20.67	5.6 ± 1.5	41.32	1.616	0.014	0.602	2.477
	a	19.87	3.4 ± 1.5	39.73	1.643	0.008	0.635	
	e	19.59	7.3 ± 2.2	39.14	1.634	0.017	0.617	
	e	19.20	7.8 ± 2.2	38.36	1.641	0.018	0.623	
	a [c]	20.466	3.1	40.93	1.623	0.008	0.615	2.504
	a [c]	19.752	2.5	39.45	1.637	0.006	0.631	
	e [c]	19.513	5.3	39.01	1.638	0.013	0.625	
	e [c]	19.207	4.9	38.40	1.644	0.011	0.633	
Bu^tCN [c]	a	20.039	2.8	40.07	1.632	0.007	0.625	2.523
	a	19.426	1.3	38.85	1.644	0.003	0.641	
	e	18.981	7.8	37.92	1.645	0.018	0.627	
	e	18.859	8.1	37.68	1.648	0.018	0.630	
Me_2C	a	20.09	1.2 ± 0.8	40.17	1.632	0.003	0.629	2.524
	a	19.48	1.2 ± 0.8	38.96	1.644	0.003	0.641	
	e	19.43	7.3 ± 1.3	38.82	1.637	0.017	0.620	
	e	18.84	6.6 ± 1.2	37.65	1.649	0.015	0.634	
MeOH	a	20.32	2.1 ± 0.4	40.64	1.627	0.005	0.622	2.525
	a	19.87	3.1 ± 0.5	39.73	1.634	0.0075	0.627	
	e	17.87	13.1 ± 1.5	35.63	1.661	0.028	0.633	
	e	17.50	12.2 ± 0.1	34.91	1.669	0.026	0.643	
EtOH	a	20.57	3.8 ± 1.5	41.13	1.620	0.009	0.611	2.455
	a	20.12	3.9 ± 1.2	40.23	1.629	0.010	0.619	
	e	17.75	19.4 ± 3.5	35.27	1.657	0.042	0.615	
	e	17.50	23.2 ± 3.2	34.69	1.659	0.049	0.610	
$C_4H_8(CN)_2$	a	20.30	1.8 ± 0.5	40.60	1.623	0.004	0.623	2.502
	e	19.06	7.1 ± 1.8	38.08	1.644	0.016	0.628	
$SeOCl_2$ [a]	a	17.030	39.5 ± 0.2	33.219	1.657	0.080	0.577	2.394
	e	19.551	6.9 ± 0.3	39.069	1.636	0.016	0.620	
$BrCH_2COOMe$	a	21.91	1.7 ± 0.5	43.82	1.598	0.005	0.598	2.480
	a	18.57	1.7 ± 0.5	37.14	1.660	0.004	0.660	
	e	19.59(2)	9.0 ± 1.6	39.13	1.632	0.021	0.611	
$ClCH_2COOMe$	a	21.82	1.1 ± 0.5	43.64	1.601	0.003	0.601	2.487
	a	18.53	1.7 ± 0.5	37.06	1.660	0.004	0.660	
	e	19.51(2)	9.0 ± 0.8	38.97	1.634	0.021	0.613	

Note. The results of Zeeman analysis of single crystals: [a] at 297 K;[45] [b] at 293 K;[44] [c] at 235 K.[46]

For the latter compounds, the results of X-ray study are consistent with those of NQR measurements: their axial Sn–Cl bond distances were found to be shorter than the equatorial ones. However, it is clear that the EFG asymmetry parameter on the chlorine atom will increase, if this atom is involved in additional (inter- or intramolecular) interactions, as it is observed in $SnCl_4(SeOCl_2)_2$.[45] The respective ^{35}Cl frequency in the NQR spectrum of the adduct decreased, and the ratios between the axial–equatorial resonance frequencies and Sn–Cl bond distances were inverted (Table 8).

The spectroscopic regularities found for the isomeric chloro adducts are not universal. Tin tetrabromide and tetraiodide adducts show different positional order of the NQR frequencies assigned to axial and equatorial halogen atoms due to different relationships between the electron-donating (withdrawing) properties of ligands L and halogens and relatively lesser contribution to the EFG of crystal-field effects as compared to the contribution of their own valence orbitals. This is illustrated in the results of NQR studies of hexacoordinate adducts $SnBr_4L_2$.[23] Although the ^{81}Br frequency ranges assigned to axial and equatorial Br atoms in the NQR spectra of *cis*-isomers also did not overlap (Table 9), their mutual positions were inverted with respect to those in the ^{35}Cl NQR spectra of the chloro analogues, *i.e.*, the ^{81}Br NQR frequencies of axial bromine atoms were lower than those of equatorial in all the *cis*-isomers studied: $112 < \nu_a < 126$ MHz; $128 < \nu_e < 142$ MHz. In agreement with the NQR data, the results of X-ray studies available for the *cis*-$SnBr_4L_2$ adducts gave axial Sn–Br bond distances exceeding the equatorial ones.[23] In the spectra of *trans*-isomers, the ^{81}Br NQR frequency range was relatively larger than the corresponding ^{35}Cl frequency range in the spectra of chloro adducts, the former interval covering almost the entire ($\nu_e + \nu_a$) frequency range of *cis*-isomers:

Table 9. ^{81}Br frequencies in the NQR spectra of isomers of hexacoordinate adducts of tin tetrabromide at 77 K.[23]

L	ν /MHz	L	a/e	ν /MHz
trans-Isomers		*cis*-Isomers		
TMU	125.30(2)	bipy	a	119.07
	123.68		a	118.67
	123.47		e	128.78
DMF	124.57			
	122.18	$NC(CH_2)_4CN$	a	130.95(2)
DPF	125.22		a	140.96
	124.72		e	141.29
DBS	127.63			
	127.18	DESO	a	118.24
Diox	136.20		e	127.07
py	122.66			
2,3-Mepy	119.54(2)	DPSO	a	116.63
	117.26		e	128.34
	115.74			
TPPO	127.91	DMSO	a	118.17
	121.14		e	127.73
HMPT	127.73			
Et_2O	135.31	CH_3OH	a	120.90
	135.58		a	125.75
Me_2O	135.82		e	135.55
	136.47		e	140.46
	136.72			
	137.27	C_2H_5OH	a	113.83(2)
THF	128.28		e	140.51
	131.26		e	141.44
	134.30			
	135.93	$(C_2H_2Ph)_2CO$	a	112.57
			e	133.62

Note. DPF is diphenylformamide; DESO is diethyl sulfoxide; relative intensities of resonance lines are given in parentheses.

$115 < \nu_e < 138$ MHz. Thus, the ^{81}Br NQR frequency ranges in the spectra of *cis- and trans*-isomers of the $SnBr_4L_2$ adducts were found to overlap. This implies that, unlike in the related chloro adducts, the EFG asymmetry parameters at the Br nuclei in the bromo adducts should be measured for the spectroscopic identification of isomerism. The mutual position of the ^{81}Br frequency ranges assigned to axial–equatorial bromine atoms indicates the prevailing electronic influence of ligands on the electron density redistribution in *cis*- and *trans*-isomers of the adducts $SnBr_4L_2$.

As a whole, the NQR results on isomers of hexacoordinate adducts $SnHal_4L_2$ show[9, 11, 18, 23] that the measurement of the EFG asymmetry parameters along with examination of the spectroscopic shifts, splittings and temperature dependence of the resonance frequencies made it possible to identify the type of isomerism of the adducts from their NQR spectra, even though the latter exhibit complicated patterns of the shifts and splittings. The average NQR frequency shifts at halogen atoms in adducts with respect to their frequencies in parent $SnHal_4$ can serve as a measure of the strength of the adducts formed provided the resulting increase in the halogen σ-electron density in the acceptor is mainly due to intramolecular electronic effects, the contributions of the crystal-field effects being much less significant.

Table 10 lists the ^{35}Cl NQR spectroscopic parameters for trigonal-bipyramidal adducts of tin(IV) having the coordination number 5. The corresponding spectra differ notably from those for pseudooctahedral adducts (Tables 7 and 8). They comprise the triplets from equatorial Cl atoms at frequencies slightly different from those of the parent tetrachloride, and the singlets from axial chlorine atoms, shifted considerably to lower frequencies, which indicates that the electron density in such adducts is mainly transferred from the ligands L to the axial chlorine atoms.

In both trigonal-bipyramidal and pseudooctahedral adducts, the asymmetry parameters on equatorial chlorine atoms exceed those on the axial atoms and vary within similar limits. Accordingly, the corresponding valence $3p_\pi$ orbital occupancy differences are also close to each other. The main difference between these two types of adducts consists of the magnitudes of the $3p_\sigma$ orbital occupancies (Np_z) at equatorial chlorine sites. In trigonal-bipyr-

Table 10. ^{35}Cl NQR spectroscopic parameters for pentacoordinate adducts of tin tetrachloride at 77 K and the M–Cl bond characteristics.[9]

L	a/e	ν /MHz	η (%)	Np_σ	ΔNp_π	$-\rho$ /e	$\lvert\sum\rho\rvert$ /e
$MeNO_2$	e	24.39	10.6 ± 0.7	1.540	0.031	0.509	2.145
	e	24.26	14.0 ± 1.2	1.537	0.041	0.496	
	e	24.01	8.4 ± 0.4	1.550	0.025	0.525	
	a	20.21	4.5 ± 0.6	1.626	0.011	0.615	
4-MeC_6H_4COCl	e	23.34	14.2 ± 1.0	1.555	0.040	0.515	2.192
	e	23.89(2)	9.6 ± 1.0	1.551	0.028	0.523	
	a	19.91	1.5 ± 0.5	1.635	0.004	0.631	
PhMe	e	23.85	12.0 ± 1.0	1.548	0.035	0.513	2.189
	e	23.66	9.2 ± 1.0	1.556	0.026	0.530	
	e	23.39	13.3 ± 1.0	1.555	0.038	0.517	
	a	20.18	0.9 ± 0.5	1.631	0.002	0.629	
2,5-$Me_2C_6H_3OMe$	e	23.90	13.0 ± 3.0	1.546	0.038	0.508	2.192
	e	23.56	12.5 ± 3.0	1.553	0.036	0.517	
	e	23.19	10.5 ± 3.0	1.563	0.030	0.533	
	a	20.11	0.0	1.634	0.0	0.634	
C_5H_5COCl	e	24.22	5.5 ± 2.0	1.551	0.016	0.535	2.205
	e	21.38(2)	4.6 ± 1.5	1.548	0.014	0.534	
	a	21.04	0.9 ± 0.5	1.604	0.002	0.602	
$SnCl_4$ [a]		24.30	2.9 ± 0.5				
		24.23	2.9 ± 0.5				
		24.14	2.9 ± 0.5	< 1.557	> 0.02	$\lvert < 0.54 \rvert$	< 2.15
		23.72	2.9 ± 0.5				

[a] Data from Ref. 47.

amidal adducts, the absolute values of Np_z are by 0.1 lower than those in the pseudooctahedral adducts, whereas the spectroscopic and electronic characteristics of their Sn−Cl axial bonds differ insignificantly. As is seen from Tables 7, 8 and 10, the overall effective charge $|\sum \rho|$ on all the chlorine atoms in the octahedral adducts is markedly larger than that in the parent tetrachloride $SnCl_4$, while in trigonal-bipyramidal adducts, the corresponding difference is small. This supports a conventional idea of relatively larger extent of charge transfer in octahedral adducts. The NQR data on pseudooctahedral adducts show that the overall σ-electron density on chlorine atoms in *trans*-isomers is on average slightly higher than that in *cis*-isomers.

IV. Penta- and hexacoordinate adducts of silicon and germanium tetrachlorides

The ^{35}Cl NQR spectroscopic parameters and M−Cl bond characteristics in adducts MCl_4L (M = Si, Ge) are summarised in Table 11, which clearly demonstrates the similarities of the spectral patterns to those of the related tin compounds: the NQR spectra of the adducts of all three elements consist of triplets from equatorial atoms, slightly shifted relative to the frequencies of parent tetrachlorides MCL_4, and lower-frequency singlets from axial chlorine atoms. However, the electronic characteristics of equatorial M−Cl bonds in adducts of different central metals M are markedly different. Thus η on the equatorial chlorine atoms was found to increase considerably in the order: Sn < Ge < Si. In silicon adducts, this increase was accompanied by a fall of the ^{35}Cl frequencies with respect to both the germanium and tin adducts and CCl_4, which can be accounted for by an increase in the π-character of the Si−Cl bonds. The participation of the chlorine $3p_\pi$ orbitals in bond formation results in their reduced occupancies Np_x and Np_y, whose sign in equation (1) is opposite to that of the $3p_\sigma$ orbital occupancy Np_z. This causes a decrease in both U_p and frequency with respect to those for the purely σ-bonded chlorine atom. In the latter case, the value of e^2Qq_{zz}/h becomes a measure of the chlorine valence $3p_\sigma$ orbital occupancy. One cannot make an independent estimation of the M−Cl bond σ- and π-characters, *i.e.*, determine three unknowns, σ, π_x and π_y from two equations (1) and (2). A spatial arrangement of ligands is however possible where the central atom M can interact with only one chlorine p_π orbital ($3p_x$), the occupancy of the other ($3p_y$) remaining undisturbed ($Np_y = 2$). Denoting $\pi_x = \pi$, we obtain equation (2) in the form

$$\eta = \frac{3\pi}{2U_p}, \tag{5}$$

so that η becomes a measure of the M−Cl π-bonding. One can now determine both parameters, σ and π, from equations (1) and (5). Such an arrangement is often the case in trigonal-bipyramidal adducts MCl_4L. The estimation of their M−Cl bond σ- and π-characters (Table 11) shows that in the silicon adducts the decrease in the equatorial ^{35}Cl frequency and increase in η result from substantial increase in the Si−Cl π-bonding. In the germanium adducts, the π-bonding is relatively weaker, whereas in $SnCl_4L$ the η values exhibit a further considerable fall. They comprise a significant contribution from external charges, which is more pronounced than in analogous germanium and silicon adducts because of the larger Sn−Cl bond ionicity. This is supported by relatively higher values of η on axial Cl atoms in comparison with equatorial in the $SnCl_4L$ adducts than in related silicon and germanium adducts.

Table 11. ^{35}Cl NQR spectroscopic parameters for pentacoordinate adducts of silicon and germanium tetrachlorides at 77 K and the M−Cl bond characteristics.[47]

Compound	a/e	ν /MHz	η (%)	e^2Qq_{zz}/h /MHz	Np_σ	ΔNp_π	$-\rho$ /e	$\lvert\sum\rho\rvert$ /e
$SiCl_4 \cdot Me_3N$	e	21.50	42.1 ± 7.2	41.78	1.566	0.107	0.459	2.081
	e	21.30(2)	36.6 ± 4.0	41.68	1.574	0.093	0.481	
	a	18.86	1.7 ± 0.5	37.77	1.654	0.004	0.650	
$SiCl_4 \cdot TMU$ [a]	e	21.65	43.1 ± 4.1	42.02	1.562	0.110	0.452	2.248
	e	21.16	38.8 ± 2.6	41.30	1.575	0.097	0.478	
	a	18.45	7.5 ± 2.0	36.86	1.656	0.017	0.639	
	a	17.34	1.7 ± 0.5	34.68	1.682	0.003	0.679	
$SiCl_4$		20.464	2.9 ± 0.5					
		20.415	2.9 ± 0.5	40.77	< 1.59	> 0.07	| < 0.52|	< 2.08
		20.408	2.9 ± 0.5					
		20.273	2.2 ± 0.5					
$GeCl_4 \cdot Me_3N$	e	24.83(2)	25.3 ± 3.9	48.92	1.516	0.075	0.441	1.948
	e	24.66	24.1 ± 3.3	48.85	1.519	0.071	0.448	
	a	20.59	2.0 ± 0.9	41.17	1.623	0.005	0.618	
$GeCl_4 \cdot TMU$	e	25.09	26.4 ± 5.0	49.06	1.510	0.079	0.431	1.914
	e	24.86	25.3 ± 4.2	49.19	1.514	0.076	0.438	
	e	24.34	27.0 ± 3.8	48.10	1.522	0.079	0.443	
	a	20.67	5.6 ± 1.0	41.33	1.616	0.014	0.602	
$GeCl_4 \cdot HMPA$	e	24.92	31.8 ± 5.0	49.02	1.506	0.095	0.411	1.890
	e	24.66	28.0 ± 4.3	48.69	1.515	0.083	0.432	
	e	24.57	28.0 ± 4.3	48.51	1.516	0.083	0.433	
	a	20.53	3.4 ± 0.5	41.05	1.622	0.008	0.614	
$GeCl_4$		25.745	2.2 ± 0.5					
		25.739	2.2 ± 0.5	51.32	< 1.51	> 0.04	| < 0.47|	< 1.89
		25.715	2.2 ± 0.5					
		25.450	2.2 ± 0.5					
		25.745 [b]	−					
		25.735 [b]	7.8					
		25.713 [b]	3.7	−	−	−	−	−
		25.449 [b]	3.4					

Note. [a] The ligand TMU is located in the equatorial plane of the adduct. [b] The results of Zeeman analysis of a single crystal at 77 K.[48]

Table 12. ^{35}Cl and ^{81}Br Frequencies (ν) in the NQR spectra of pseudooctahedral adducts of silicon and germanium tetrachlorides and EFG asymmetry parameters (η) at 77 K.

L	e/a	ν /MHz	η (%)
$SiCl_4L_2$			
trans-py	e	19.15	6.6 ± 0.6
trans-TPPO	e	18.29	
cis-4,4′-Me_2-α,α-bipy	e	19.03(2)	13.0 ± 1.0
	a	18.4	2.0 ± 0.7
$GeCl_4L_2$ (see Ref. 49)			
trans-py	e	20.45	6.7 ± 1.0
trans-HMPT	e	21.10	7.8 ± 1.2
trans-DMF	e	20.67	8.2 ± 0.8
	e	20.32	{5.7}
cis-DMSO	e	20.82	{13.0}
	a	19.69	
cis-DESO	e	20.56	
	a	19.59	
$GeBr_4L_2$ (see Ref. 49)			
trans-py	e	139.78	
HMPT	–	135.09	
		146.46	
DMF	–	138.43	
		145.46	

Only a few results of NQR studies are currently available on pseudooctahedral adducts of silicon and germanium tetrahalides (Table 12), most important being the value of the asymmetry parameter η on the chlorine atoms in the only *cis*-isomer of the adduct $SiCl_4L_2$.This enables one to assign the ^{35}Cl NQR frequencies to equatorial and axial chlorine atoms and find that their positional order on a frequency scale is inverted with respect to that in analogous tin adducts: unlike in the latter, the lower-frequency components in the spectra of silicon adducts are assigned to axial Cl atoms. Unfortunately, lack of data on *cis*-isomers does not allow one to conclude whether this order is typical of silicon adducts.

Table 13 lists the M–Hal bond characteristics and effective charges on halogen sites in all the spectroscopically examined pseudooctahedral (MCl_4L_2) and trigonal-bipyramidal (MCl_4L) adducts of silicon and germanium tetrachlorides. The corresponding characteristics for $SnCl_4L_2$ and $SnCl_4L$ averaged over all the known examples are also included in the table. One can see that the chlorine $3p_\pi$ orbital occupancy differences at equatorial sites ($\Delta Np_\pi = Np_x - Np_y$) in all the hexacoordinate adducts MCl_4L_2 (M = Si, Ge, Sn), are close to each other, the main difference between the adducts consisting in the chlorine $3p_\sigma$ orbital occupancies. The absolute magnitudes of the effective charge ρ on the equatorial chlorine atoms vary in the order: Sn ~ Si > Ge. When the adduct of pseudooctahedral configuration is compared to that of trigonal-bipyramidal geometry, one can find that the axial M–Cl bond characteristics differ insignificantly in both types of the adducts, whereas the equatorial bonds are markedly different, the difference being determined by the nature of the central atom. The effective negative charge on the equatorial chlorine atom increases in absolute value as the coordination number of the central atom increases (Table 14). In the tin adducts, this increase in the charge is nearly fully induced by the increase in chlorine $3p_\sigma$ orbital occupancy, whereas in the germanium and especially in the silicon adducts, it is provided by both the increased chlorine $3p_\sigma$ orbital occupancy and reduced ΔNp_π. This may be accounted for by the increased local symmetry of the Cl site in a crystal as well as the M–Cl bond elongation accompanying an increase in the coordination number. In germanium tetrachloride adducts, the contributions of the $3p_\sigma$- and $3p_\pi$-systems to the effective charge increment on the Cl atom amount in absolute magnitude to 0.104 and 0.059, respectively; in the silicon adducts, the contribution of the chlorine $3p_\pi$ orbitals to the respective increment exceeds that of the $3p_\sigma$ orbitals (0.079 and 0.069, respectively).

Table 13. Average effective charges ($-\rho$) on chlorine atoms and chlorine valence $3p$ orbital occupancies ($Np_\sigma = Np_z$, $\Delta Np_\pi = Np_x - Np_y$) in adducts MCl_4L and MCl_4L_2.

M	Atom	a/e	Np_σ	ΔNp_π	$-\rho$ /e
MCl_4L_2					
Sn	Cl	e	1.645	0.025	0.620
	Cl	a	1.624	0.007	0.617
Ge	Cl	e	1.614	0.021	0.593
	Cl	a	1.641	0.0	0.641
Si	Cl	e	1.641	0.023	0.618
	Cl	a	1.662	0.005	0.657
MCl_4L					
Sn	Cl	e	1.550	0.029	0.521
	Cl	a	1.627	0.005	0.622
Ge	Cl	e	1.510	0.080	0.430
	Cl	a	1.619	0.009	0.610
Si	Cl	e	1.572	0.102	0.470
	Cl	a	1.654	0.004	0.650

Table 14. Average values of effective charges on equatorial chlorine atoms and chlorine valence $3p$ orbital occupancies in adducts MCl_4L and MCl_4L_2 and variations of their absolute magnitudes (δp, δNp_σ, $\delta\Delta Np_\pi$) due to the change $MCl_4L \rightarrow MCl_4L_2$.

Adduct	$-\rho$(Cl) /e	Np_σ	ΔNp_π	$\delta\rho$ /e	δNp_σ	$\delta\Delta Np_\pi$
$SiCl_4L \rightarrow SiCl_4L_2$						
$SiCl_4L$	0.470	1.572	0.102	+0.148	+0.069	−0.079
$SiCl_4L_2$	0.618	1.641	0.023			
$GeCl_4L \rightarrow GeCl_4L_2$						
$GeCl_4L$	0.430	1.510	0.080	+0.163	+0.104	−0.059
$GeCl_4L_2$	0.593	1.614	0.021			
$SnCl_4L \rightarrow SnCl_4L_2$						
$SnCl_4L$	0.521	1.550	0.029	+0.099	+0.095	−0.004
$SnCl_4L_2$	0.620	1.645	0.025			

Thus, the NQR data available on the trigonal-bipyramidal $SiCl_4L$ and $GeCl_4L$ adducts provide evidence that the $3p_\pi$-systems of the equatorial Si–Cl and Ge–Cl bonds contribute considerably to the bond formation, the estimated π-character amounting on average to 0.1 and 0.08, respectively. It should be noted however that the NQR data enable one to compare an extent of participation of the equatorial chlorine $3p_\pi$ electrons in the M–Cl bonding, whereas the question of the mechanism of the π-interaction remains open. In addition, the magnitude of ΔNp_π may not be a measure of the M–Cl bond π-character in pseudooctahedral adducts $SiCl_4L_2$ and $GeCl_4L_2$, if the electron density is withdrawn from both chlorine $3p_\pi$ orbitals; in this case, the true extent of the π-character will be higher than that estimated from ΔNp_π. This also holds for the parent tetrachloride molecules having slightly distorted tetrahedral structures.[48]

The variation of the chlorine valence p orbital occupancies upon adduct formation was discussed based on the results of PM3 calculations of model acceptor molecules and adducts MCl_4L and MCl_4L_2 (M = Si, Ge, Sn).[37,38] The M–Cl bond π-character was

identified by the authors with the magnitude of ΔNp_π determined in the parent tetrachlorides by the NQR experiments.[47]

For $SiCl_4$ and $GeCl_4$, such an estimation gave $\pi = 0.007$, which resulted in the considerably overestimated absolute value of the negative effective charge on the chlorine atom: $\rho(Cl) = 0.618$ and 0.525 e in $SiCl_4$ and $GeCl_4$, respectively. Hence, the entire charge on the chlorine atoms $|\sum \rho(Cl)|$ was 2.472 e in $SiCl_4$ and 2.1 e in $GeCl_4$, which notably exceeded in absolute magnitude the appropriate charges in adducts MCl_4L, namely, 1.983 e in $SiCl_4 \cdot NMe_3$ and 1.912 e in $GeCl_4 \cdot NMe_3$.

The contradictions arisen were accounted for[37,38] by the difference between the symmetry of free MCl_4 molecules (T_d) and the symmetry of the same molecules in the adducts (D_{3h} in MCl_4L and D_{4h} in MCl_4L_2). The results of PM3 calculations showed that the total effective charge on the chlorine atoms $|\sum \rho(Cl)|$ in hypothetical MCl_4 molecules, whose symmetry and M–Cl bond distances are the same as those in the corresponding adducts, was reduced as a result of the molecular spatial rearrangement only (the charge transfer being ignored) up to 2.184 e in $SiCl_4$ and 1.988 e in $GeCl_4$. However, it is to be noted that similar characteristics ($|\sum \rho(Cl)|$) of the MCl_4 molecules in the adducts $SiCl_4 \cdot NMe_3$ and $GeCl_4 \cdot NMe_3$ estimated from the orbital occupancies using the PM3 approach[37,38] decrease accordingly:

Atom	a/e	Np_z	$Np_x + Np_y$	$Np_x - Np_y$	$-\rho$ /e	$\sum \rho(Cl)$ /e
$SiCl_4 \cdot Me_3N$						
Cl	a	1.579	3.911	0.016	0.490	1.504
Cl	e	1.440	3.898	0.044	0.338	–
$GeCl_4 \cdot Me_3N$						
Cl	a	1.481	3.903	0.019	0.384	1.176
Cl	e	1.381	3.883	0.055	0.264	–

One can see that the calculated η values at the equatorial Cl atoms in the adducts in question (16.4% in $SiCl_4 \cdot NMe_3$ and 20.7% in $GeCl_4 \cdot NMe_3$)[37,38] do not reflect even qualitatively the trends observed in experiments (see the measured magnitudes of η in Table 11).[47] Hypothetical molecules MCl_4 having the D_{4h} symmetry and M–Cl bond distances characteristic of those in pseudooctahedral adducts MCl_4L_2 were calculated to give the largest values of η at the chlorine atoms, namely, $\eta \approx 31\%$ in $SiCl_4$, 37% in $GeCl_4$ and 33% in $SnCl_4$.[37,38] Meanwhile, the experimental **Z** values at chlorine atoms did not exceed 15% in any of the measured MCl_4L_2 adducts (Tables 7 and 8), unless this atom is involved in secondary inter- or intramolecular interactions, as in the adducts $SnCl_4(SeOCl_2)_2$ and $SnCl_4(EtOH)_2$ (Table 8). Moreover, the average values of η at the equatorial chlorine atoms in the adducts $SiCl_4L_2$ and $GeCl_4L_2$ are notably lower than in the related trigonal-bipyramidal adducts $SiCl_4L$ and $GeCl_4L$.

There is no question that spatial reconstruction of an acceptor molecule upon complexation is accompanied by electron density redistribution. However, the orbital occupancies calculated within the PM3 approximations do not account for the inconsistency between the effective charges on the chlorine atoms in free acceptor molecules and their adducts,[37,38] nor the reasons for the increase in the π-character of the M–Cl equatorial bonds in the adducts MCl_4L (Sn < Ge < Si) found in NQR experiments.[47]

But no inconsistency arises if one takes into account that the T_d symmetry of the parent tetrachloride molecules allows for the participation of both chlorine $3p_\pi$ orbitals in bond formation, whereas one can measure by NQR only the difference between their occupancies. Let us take the values of Np_x and Np_y in $SiCl_4$ (fitting the measured NQR frequencies and η), which give rise to the Si–Cl bond π-character typical of the equatorial Si–Cl bonds in the adducts $SiCl_4L$ (for example, $\pi = 0.093$, $Np_x = 1.957$, $Np_y = 1.950$). One can find herefrom that the corresponding effective charges on the Cl atoms in the $SiCl_4$ molecules ($\rho = -0.49$ e, $\sum\rho(Cl) = -1.96$ e) are consistent with those in the $SiCl_4L$ adducts ($-2.1 > \sum\rho(Cl) > -2.3$ e, see Table 11), hence allowing for the charge transfer from the ligand L to the acceptor $SiCl_4$.

The problem of electron density distribution in Main Group IV element chloro complexes has received much attention in Refs 34–39. The results of semiempirical quantum-chemical calculations were reported, and their conformity to the data obtained using the NQR, Mössbauer and X-ray fluorescence spectroscopies were discussed. It was found that upon complexation, the positive charge on the central atom of the acceptor molecule increases with respect to that in the free MCl_4 molecule, which is in agreement with the results of other publications.[43] It was however noted that according to the X-ray fluorescence spectroscopy data (ClK_α-shifts), the electron density on the chlorine atoms in the adducts MCl_4L_2 either remains unchanged or decreases as compared to free MCL_4. The reader is referred to a review[43] where the criticism of this conclusion was given.

The quantum-chemical calculations of the trigonal-bipyramidal adducts $SiCl_4 \cdot NMe_3$ (**5**), $SiCl_4 \cdot CO(NMe_2)_2$ (**6**) and pseudooctahedral $SiCl_4 \cdot (py)_2$ adduct (**7**) were made within the MNDO approximations.[49–52] The changes in silicon, nitrogen, oxygen and chlorine valence p orbital occupancies as well as the effective charges on the appropriate atoms were considered as functions of the reaction coordinate of complexation, the considered separation between the components of the adducts varying from infinity ($d = 200$ Å) to 1.5 Å. As the calculated heats of formation showed, the most energetically favourable structures of **5** and **6** were those with the ligand L in axial and equatorial positions of the bipyramid, respectively, which is in agreement with their ^{35}Cl NQR spectral patterns (Table 11).

When the shape of the $SiCl_4$ molecule changes from tetrahedral to that in the adduct **5** (at $d = 200$ Å), the effective charge on the silicon atom decreases in absolute magnitude by 0.116 e, and that on the equatorial chlorine atom, by 0.059 e, whereas the absolute magnitude of the negative charge on the axial chlorine atom increases by 0.061 e. When the components of **5** approach each other to reach $d = 2.25$ Å, at which distance the heat of adduct formation is a minimum, the effective charge on silicon begins to grow. At the same time, the negative charge on nitrogen decreases and that on chlorine, increases in absolute value, the increment being larger on the equatorial Cl atoms. It was estimated[50,52] that the formation of **5** results in the transfer of electron density of 0.2 e from the donor (mainly, from the nitrogen lone pair p_x orbital) to the acceptor (mainly, to the equatorial chlorine p_σ orbitals) molecule, which is in good agreement with experiment.[47] However, low sensitivity of this semiempirical method to the chlorine $3p_\pi$ orbital occupancies was noted. The calculated differences between the equatorial chlorine $3p_x$ and $3p_y$ orbital occupancies in the adduct **5** were negligibly small, whereas the experimental asymmetry parameters η on these atoms were large, the corresponding ΔNp_π values contributing considerably to the effective charge values (Table 11). Thus, the estimation of the effective charge on chlorine atoms from the calculated orbital occupancies[50,52] is not quite reliable.

A similar calculation for the adduct **6**[51,52] with a tetramethylurea ligand occupying an equatorial position shows that the formation of **6** also results in the transfer of the charge from the donor to chlorine atoms of the acceptor molecule, but in this case, the electron density is mainly transferred to the axial chlorines. The donor atoms are carbon of the carbonyl group, one of the nitrogen atoms and hydrogens from the dimethylamino groups, both p_σ and p_π orbitals of the carbonyl group contributing to the charge transfer. An increase in positive charge on silicon and in negative charge on oxygen upon adduct formation is caused presumably by polarisation of the Si–Cl and Si–O bonds.[51,52] The p_σ orbital occupancies of the axial (1.591 e) and equatorial (1.523 e) chlorine atoms in **6**, found by the MNDO calculations, are in agreement with the observed trends (Table 11), while the

values of Np_x and Np_y at the equatorial chlorine atoms showed, as in **5,** poor agreement with experiment.[47]

The results of MNDO calculations of **5**, **6** and pseudooctahedral **7** adducts were summarised [52] to conclude that the formation of all the three adducts results in an increase in positive charge on the silicon atom, the conclusion being supported by the Mössbauer and X-ray fluorescence spectroscopy data [34–36] available on the adducts of Main Group IV element tetrachlorides. The increasing charges, positive on silicon and negative on nitrogen, gave the authors [52] grounds to believe that the electrostatic interactions resulting in polarisation of the bonds contribute considerably into the electron density distribution upon complexation. The electrostatic interactions initiate the charge transfer: the estimated total charge located on the acceptor fragment of the adduct was negative (−0.523 e in **7**) and that on the donor fragments, positive (+0.206 e per pyridine ring in **7**).

In order to compare the chlorine orbital occupancies calculated within the MNDO approximations with those derived from the NQR experiment the assumption was made [52] (in the absence of the published η values) that the values of η at the equatorial chlorine atoms in pseudooctahedral adducts $SiCl_4L_2$ are similar to those for trigonal-bipyramidal adducts $SiCl_4L$. Thus, the value $\eta = 0.4$, which is the average for the $SiCl_4L$ adducts, was used to estimate Np_x (at $Np_y = 2$) at the equatorial Cl atoms in **7**. This gave $Np_x = 1.909$ and $\Delta Np_\pi = 0.09$, the latter being considerably overestimated compared to the correct value $\Delta Np_\pi = 0.015$ derived from the recently measured η in $SiCl_4 \cdot 2py$. As was noted above, the values of ΔNp_π at the equatorial chlorine atoms, derived from the NQR spectra of $SiCl_4L_2$ and $GeCl_4L_2$, are markedly lower than those in analogous trigonal-bipyramidal adducts. But even this correct magnitude of ΔNp_π exceeded considerably the value $\Delta Np_\pi = 0.004$ (and hence $\eta = 0.016$) found by the MNDO calculations.[52] Therefore, for the pseudooctahedral adduct **7**, the MNDO approach also gave an η value in poor agreement with experiment (Tables 11 and 12).

It was however reported [53] that the results of calculations of η can be in much better agreement with the experiment if one takes into account that the EFG (q_{zz}, q_{xx}, q_{yy}) at the quadrupole atom is produced not by its entire valence p shell, but its less diffuse part which can be determined by *ab initio* calculations of a large number of molecules in the split valence basis set 6-31G* using full optimisation of the molecular geometry.

It is reasonable to discuss how the differences in the M−Cl bond characterisitics influence the formation by silicon, germanium and tin tetrachlorides of pentacoordinate adducts with ligands of various donating power. Before discussing this problem, the bonding in the parent tetrachlorides should be considered in more detail. Note once more that the values of η measured in tetrahedral MCl_4 molecules and octahedral adducts MCl_4L_2 using spin-echo technique and powder samples [9, 47] were in agreement with those measured with single crystals of similar compounds,[44–46, 48] whereas earlier experiments [54, 55] using continuous-wave techniques for measuring η with powder samples of MCl_4 (M = Si, Ge, Sn), yielded the asymmetry parameters η, whose values were an order of magnitude higher than those given in Tables 10 and 11, which is unlikely on symmetry grounds. An independent estimation of the M−Cl bond σ- and π-characters from equations (1) and (2) is impossible in these molecules, because η at chlorine sites is equal to zero ($Np_x = Np_y$), and two unknowns, σ and π, remain in equation (1). The probable intervals for the values of M−Cl bond σ- and π-characters in MCl_4 were found based on the data obtained for the adducts MCl_4L.[47] The magnitude of the entire effective charge $|\sum\rho(\mathrm{Cl})|_{MCl_4}$, born by all the chlorine atoms in the parent molecule MCl_4, was varied with respect to the related value for the adducts $|\sum\rho(\mathrm{Cl})|_{MCl_4}$, assuming that the latter is at least no less than the former: in fact, an increase in the entire effective charge on the chlorine atoms $|\sum\rho(\mathrm{Cl})|_{MCl_4}$, depending on the amount of charge transferred from the donor L, is normally observed upon adduct formation.

For the silicon compounds, the results of varying the difference $\Delta = |\sum\rho(\mathrm{Cl})|_{SiCl_4L} - |\sum\rho(\mathrm{Cl})|_{SiCl_4}$ showed that the strengthening of the equatorial Si−Cl bonds by virtue of both σ and π orbitals is expected in the adduct with respect to $SiCl_4$ as Δ varies in the interval $0 < \Delta < 0.18$ e (Table 15). This implies that if the extent of charge transfer from the ligand L is small (due, for instance, to the weak donating power of ligands L), the adduct formation will be accompanied by an additional charge transfer from the equatorial chlorine atom σ and π orbitals to the axial ones. When the extent of charge transfer is increased, so that Δ varies in the interval $0.18 < \Delta < 0.21$ e, weakening of the equa-

Table 15. Variation of chlorine valence $3p_z$ orbital occupancies (δNp_σ) and equatorial M−Cl bond π-character ($\delta\pi$) in adducts MCl_4L in relation to the difference Δ between the total effective charges on the chlorine atoms in the adduct and parent tetrachloride MCl_4.

Compound	$\sum\rho$(Cl) /e	−ρ(Cl) /e	a/e	Np_σ	π	Δ /e	δNp_σ	δπ
$SiCl_4L$	2.07	0.473	e	1.571	0.098			
		0.650	a	1.654	0.004			
$SiCl_4$	2.07	0.517	–	1.591	0.074	0.0	−0.020	+0.024
	1.96	0.490	–	1.582	0.092	0.11	−0.011	+0.006
	1.924	0.481	–	1.579	0.098	0.146	−0.008	0.0
	1.89	0.472	–	1.576	0.104	0.18	−0.005	−0.06
	1.86	0.465	–	1.573	0.109	0.21	−0.002	−0.11
	1.836	0.459	–	1.571	0.113	0.234	+0.00	−0.015
	1.77	0.442	–	1.566	0.124	0.30	+0.005	−0.026
$GeCl_4L$	1.89	0.425	e	1.512	0.087			
		0.614	a	1.622	0.008			
$GeCl_4$	1.89	0.472	–	1.512	0.040	0.0	0.00	+0.047
	1.84	0.460	–	1.508	0.048	0.05	+0.004	+0.039
	1.607	0.402	–	1.489	0.087	0.283	+0.023	0.0
	1.53	0.382	–	1.482	0.100	0.36	+0.030	−0.013
$SnCl_4L$	2.15	0.511	e	1.543	0.032			
		0.615	a	1.626	0.011			
$SnCl_4$	2.15	0.537	–	1.557	0.020	0.0	−0.014	+0.012
	2.052	0.513	–	1.545	0.032	0.098	−0.002	0.0
	1.96	0.490	–	1.537	0.047	0.19	+0.006	−0.015
	1.88	0.470	–	1.531	0.061	0.27	+0.012	−0.029

torial Si−Cl bonds through the π-mechanism is expected, *i.e.*, increase in the electron density will partly localise on the equatorial chlorine atom $3p_\pi$ orbitals of the acceptor molecule being withdrawn from their $3p_\sigma$ orbitals until Δ reaches 0.21 e, after which the weakening will occur through the σ-system also.

The variation of Δ should evidently proceed within reasonable limits. The situation where the π-bonding in $SiCl_4$ exceeds the equatorial Si−Cl bond π-character in the adducts seems improbable. From the other side, the assumption of pure σ-bonds in $SiCl_4$ leads to the conclusion that the total σ-electron density in the acceptor molecule decreases considerably upon adduct formation, which is also unlikely. It thus follows that the most probable limits for variation of Δ, associated with the formation of the adducts $SiCl_4L$, are $0 < \Delta < 0.30$ e.

Similarly, strengthening of the equatorial Ge−Cl bonds in the adducts $GeCl_4L$ with respect to $GeCl_4$ is first expected as the extent of charge transfer increases within $0 < \Delta < 0.22$ e, which is then followed by their weakening at $\Delta > 0.22$ e. But unlike the silicon adducts, the Ge−Cl bond strengthening involves the π-system only, whereas the chlorine $3p_\sigma$ orbital occupancy can only increase, whatever small extent of charge transfer may be in the germanium adducts (Table 15). The range for variation of Δ associated with the formation of the adducts $GeCl_4L$ ($0 < \Delta < \sim 0.40$ e) is here larger than for the silicon adducts. As to the adducts $SnCl_4L$, their equatorial Sn−Cl bonds weaken at $\Delta > 0.13$ e.

Thus, the NQR data, if not providing the undisputable absolute magnitudes of the electronic characteristics, reveal considerable difference between the equatorial M−Cl bonds in trigonal-bipyramidal adducts of silicon, germanium and tin tetrachlorides. This difference determines specific changes in their σ- and π-components when going to the adducts of pseudooctahedral configuration. Several characteristic distinctions, depending on the nature of the central atom M and donating power of ligand L, were revealed when the electron density redistribution due to formation of pentacoordinate adducts by the parent MCl_4 molecules was compared using the NQR data.

V. Conclusion

The NQR spectroscopic data refine our understanding of the electronic effects due to substitution and spatial rearrangement of the coordination polyhedra in adducts and complexes of tin, germanium and silicon tetrachlorides. They provide information on the relative contribution of the σ- and π-systems to the electron density redistribution. The results of NQR studies of adducts and complexes of monoalkyl(phenyl)-substituted chloro, bromo and iodostannates enabled one to estimate and compare the contributions of their σ-electron systems to weakening of the Sn−Cl bonds in *cis*-positions relative to the substituents. An estimation of the effective charges on the halogen atoms in *cis*- and *trans*-positions to the substituents made it possible to compare quantitatively the contributions of *cis*-weakening and *trans*-strengthening to the resulting electron density redistribution in the adduct due to replacement of the acidoligands; participation of the halogen π-electron system in the M−Cl bond *trans*-strengthening was revealed. The NQR spectra provide evidence that the length of the chain in the alkyl groups of the substituent influences insignificantly the overall *cis*-weakening of the Sn−Cl bonds. This permitted one to estimate the contribution of the ligands L to the Sn−Cl bond weakening in the presence of the alkyl groups in dialkyldibromostannates. An examination of dependence of the EFG asymmetry parameters at the iodine atoms in the adducts of type $R_2SnI_2L_2$ on the iodine valence orbital occupancies showed that an increase of the halogen σ-electron density due to *cis*-weakening leads to an increase in η at a fixed $\Delta Np_\pi = Np_x - Np_y$ difference.

Comparison of the NQR and X-ray diffraction data enabled one to correlate on a quantitative basis the change in the Sn−Hal bond lengths with the effective charge increments on the appropriate halogen atoms. The NQR spectroscopic parameters directly determined by the electron density distribution at the halogen atoms were found to be more sensitive to the electronic effects than the interatomic distances. However, X-ray data on the spatial arrangement of atoms and atomic groups, especially in isomers, appeared to be very important for the correct assignment of resonance lines and hence correct interpretation of the NQR spectra. However, examples are known where the electronic effects registered by NQR gave structural evidences below the accuracy of X-ray experiments. Thus the structural effects of *trans*-strengthening in adducts and complexes of monoalkyl(phenyl)tin trichlorides were small, so that the corresponding *trans*-shortening was comparable with the standard deviation values, whereas the electronic effects involved were registered by NQR with an accuracy notably exceeding the errors of measurement. Similarly, no structural evidence for any intermolecular (interligand) interactions were found by X-ray in the adduct $Ph_2SnI_2(HMPT)_2$, whose ^{127}I NQR spectral patterns were consistent with a considerable disturbance of the iodine valence π-electron system caused seemingly by the π−π interactions between the iodine atom and phenyl rings of the substituents.

The measurement of the EFG asymmetry parameters at chlorine atoms in pseudooctahedral adducts $SnCl_4L_2$ enabled one to find a spectroscopic criterion of *cis*−*trans* isomerism of the adducts. The type of isomer could be identified, using this criterion, by measuring the ^{35}Cl NQR frequencies only. The identification of isomers led to better understanding of the electronic reorganisation of the adducts as a result of their rearrangement from pseudooctahedral to trigonal-bipyramidal geometry. It was found that the transformation $SnCl_4L_2 \rightarrow SnCl_4L$ is accompanied by an insignificant change in the axial Sn−Cl bond character. The equatorial Sn−Cl bond π-system also remains undisturbed by this transformation. The main influence was exerted on the equatorial halogen atom valence $3p_\sigma$ orbitals, whose occupancies decreased on average by 0.1 e.

The measurement of η at chlorine atoms in analogous adducts of germanium and silicon tetrachlorides demonstrated both similarities and differences between the M−Cl bond characteristics. According to the NQR data, the equatorial M−Cl (M = Sn, Ge, Si) bond π-character considerably increases in the trigonal-bipyramidal adducts in the order Sn < Ge < Si ($0.03 < 0.08 < 0.1$, respectively). On going from these adducts to the adducts of pseudooctahedral configuration, the axial M−Cl bond exhibits only minimal changes. However, the electron density redistribution over the σ- and π orbitals of the equatorial M−Cl bonds strongly depends on the nature of the central atom: an increase in the coordination number of the latter results in an increase in absolute magnitude of the effective charges on the equatorial chlorine atoms. In tin adducts, this increase is completely provided by the increased halogen $3p_\sigma$ orbital occupancy, whereas in the silicon adducts, the charge increment, caused by the reduced chlorine $3p_\pi$ orbital occupancy difference (0.079), exceeds that contributed by its $3p_\sigma$ orbital (0.069).

The difference between the bonds of tin, germanium and silicon tetrachlorides causes the different character of σ- and π-electron density redistribution upon formation of trigonal-bipyramidal adducts with ligands L of various donating powers.

The work was supported by the Russian Foundation for Basic Research (Project No. 96-03-34280).

References

1. Yu A Buslaev, E A Kravchenko, L Kolditz *Coord. Chem. Rev.* **82** 1 (1987)
2. K V Raman *J. Mol. Struct.* **345** 31 (1995)
3. Yu E Sapozhnikov, Ya B Yasman *Izv. Akad. Nauk SSSR, Ser. Fiz.* **42** 2148 (1978)

4. V P Feshin, Yu E Sapozhnikov, G V Dolgushin, Ya B Yasman, M G Voronkov *Dokl. Akad. Nauk SSSR* **247** 158 (1979) [a]
5. V P Feshin, G V Doldushin, M G Voronkov, Yu E Sapozhnikov, Ya B Yasman, V I Shiryaev *J. Organomet. Chem.* **295** 15 (1985)
6. V P Feshin, M G Voronkov, G V Dolgushin, P A Nikitin, I M Lazarev, Yu E Sapozhnikov, Ya B Yasman *Dokl. Akad. Nauk SSSR* **268** 1163 (1983) [a]
7. V P Feshin, G V Dolgushin, I M Lazarev, Yu E Sapozhnikov, Ya B Yasman, M G Voronkov *Dokl. Akad. Nauk SSSR* **300** 1181 (1988) [a]
8. V G Morgunov, E A Kravchenko *Pribory Tekhn. Eksper.* (6) 199 (1988)
9. E A Kravchenko, V G Morgunov, M Yu Burtsev, Yu A Buslaev *Zh. Obshch. Khim.* **60** 1945 (1990) [b]
10. E A Kravchenko, M Yu Burtsev *Z. Naturforshch., A Phys. Sci.* **47** 134 (1992)
11. V P Feshin, G V Dolgushin, I M Lazarev, M G Voronkov, E A Kravchenko, V G Morgunov, M Yu Burtsev *Dokl. Akad. Nauk SSSR* **301** 1155 (1988) [a]
12. E A Kravchenko, M Yu Burtsev *Z. Naturforshch., A Phys. Sci.* **51** 641 (1996)
13. V I Nefedov *Koord. Khim.* **1** 1299 (1975) [c]
14. N A Popov *Koord. Khim.* **2** 1155 (1976) [c]
15. A A Levin, S P Dolin *Koord. Khim.* **5** 320 (1979) [c]
16. J I Musher *J. Am. Chem. Soc.* **94** 1370 (1972)
17. E M Shustorovich, Yu A Buslaev *Koord. Khim.* **1** 1020 (1975) [c]
18. Yu A Buslaev, E A Kravchenko, M Yu Burtsev, L A Aslanov *Coord. Chem. Rev.* **93** 185 (1989)
19. P Stork, A Weiss *Ber. Bunsenges. Phys. Chem.* **94** 179 (1990)
20. D Borchers, P C Schmidt, A Weiss *Z. Naturforshch., A Phys. Sci.* **43** 643 (1988)
21. P Stork, A Weiss *Ber. Bunsenges. Phys. Chem.* **93** 454 (1989)
22. P Stork, N Weiden, A Weiss *Z. Naturforshch., A Phys. Sci.* **45** 229 (1990)
23. M Yu Burtsev, E A Kravchenko *Zh. Neorg. Khim.* **39** 1694 (1994) [d]
24. A V Yatsenko, S V Medvedev, A I Tursina, L A Aslanov *Zh. Obshch. Khim.* **56** 2330 (1986) [b]
25. E A Kravchenko, M Yu Burtsev, Yu A Buslaev *Dokl. Akad. Nauk* **340** 334 (1995) [a]
26. E A Kravchenko, M Yu Burtsev, A V Yatsenko, L A Aslanov *Main Group Metal Chem.* **20** 339 (1997)
27. V A Tafeenko, K A Paseshnichenko, H Schenk *Z. Kristallogr.* **211** 457 (1996)
28. V P Feshin, G V Dolgushin, I M Lazarev, M G Voronkov *Zh. Obshch. Khim.* **58** 2267 (1988) [b]
29. V P Feshin, G V Dolgushin, I M Lazarev, M G Voronkov *Zh. Obshch. Khim.* **59** 745 (1989) [b]
30. V P Feshin, G V Dolgushin, I M Lazarev, M G Voronkov *Zh. Obshch. Khim.* **60** 1116 (1990) [b]
31. V P Feshin, G V Dolgushin, I M Lazarev, M G Voronkov *Z. Naturforshch., A Phys. Sci.* **45** 219 (1990)
32. V P Feshin, G V Dolgushin, I M Lazarev, M G Voronkov *Koord. Khim.* **16** 1038; 1215 (1990) [c]
33. A I Andreeva, I Ya Kuramshin, A A Muratova, D Ya Osokin, A N Pudovik, I A Safin *Izv. Akad. Nauk SSSR, Ser. Fiz.* **39** 2590 (1975)
34. O Kh Poleshchuk, G N Dolenko *Zh. Strukt. Khim.* **29** (4) 177 (1988) [e]
35. O Kh Poleshchuk, B Nogaj, G N Dolenko, V P Elin *Mol. Phys. Rep.* **6** 230 (1994)
36. G N Dolenko, A L Litvin, V P Elin, O Kh Poleshchuk *Zh. Strukt. Khim.* **33** (2) 67 (1992) [e]
37. O Kh Poleshchuk, I Latoshinska *Koord. Khim.* **22** 33 (1996) [c]
38. O Kh Poleshchuk, J N Latosinska, B Nogaj *J. Mol. Struct.* **380** 277 (1996)
39. O Kh Poleshchuk, V P Elin, J Koput, B Nogaj, G N Dolenko *J. Mol. Struct.* **344** 107 (1995)
40. A I Kuz'min, G N Zviadadze *Koord. Khim.* **6** 1538 (1980) [c]
41. P G Hugett, R J Lynch, T C Waddington, K Wade *J. Chem. Soc., Dalton Trans.* 1164 (1980)
42. J Rupp-Bensadon, E A C Lucken *J. Chem. Soc., Dalton Trans.* 495 (1983)
43. V P Feshin *Main Group Metal Chem.* **16** 377 (1993)
44. M Mishima, T Okuda *Bull. Chem. Soc. Jpn.* **62** 2263 (1989)
45. M Mishima *J. Sci. Hiroshima Univ.* **A46** 41(1982)
46. M Mishima, T Okuda *Bull. Chem. Soc. Jpn.* **63** 1206 (1990)
47. Yu A Buslaev, E A Kravchenko, V G Morgunov, M Yu Burtsev, V P Feshin, G V Dolgushin, I M Lazarev, M G Voronkov *Dokl. Akad. Nauk SSSR* **301** 1408 (1988) [a]
48. S Sengupta, G Litzistorf, E A C Lucken *J. Magn. Reson.* **42** 45 (1981)
49. E A Kravchenko, M Yu Burtsev, Yu A Buslaev *Zh. Khim. Fiz.* **17** 21 (1998) [f]
50. V P Feshin, M Yu Kon'shin *Zh. Obshch. Khim.* **65** 992 (1995) [b]
51. V P Feshin, M Yu Kon'shin *Koord. Khim.* **21** 694 (1995) [c]
52. V P Feshin, M Yu Konshin *Main Group Metal Chem.* **18** 101 (1995)
53. V P Feshin, M Yu Konshin *Z. Naturforshch., A Phys. Sci.* **51** 549 (1996)
54. J Darville, A Gerard, M T Calende *J. Magn. Reson.* **16** 205 (1974)
55. J D Graybeal, P J Green *J. Phys. Chem.* **73** 2948 (1969)

[a] — *Dokl. Chem. Technol., Dokl. Chem. (Engl. Transl.)*
[b] — *Russ. J. Gen. Chem. (Engl. Transl.)*
[c] — *Russ. J. Coord. Chem. (Engl. Transl.)*
[d] — *Russ. J. Inorg. Chem. (Engl. Transl.)*
[e] — *Russ. J. Struct. Chem. (Engl. Transl.)*
[f] — *Russ. J. Chem. Phys. (Engl. Transl.)*